HYDROGEOLOGY OF A PORTION OF YOSEMITE VALLEY: GROUNDWATER AND SURFACE WATER INTERACTION AND CONCEPTUAL GROUNDWATER MODEL

Final Project Report

Prepared For:

U.S. National Park Service

Prepared By:

Nicholas J. Newcomb and Graham E. Fogg
Hydrologic Sciences Graduate Group
Department of Land, Air and Water Resources
University of California, Davis

May 2011

TABLE OF CONTENTS

EXECUTIVE SUMMARY

Introduction

As part of a 2009 court settlement, the National Park Service has agreed to complete a revised Comprehensive Management Plan for the Merced River to fulfill the requirements of National Environmental Protection Act and Wild and Scenic Act (United States District Court, 2009). In order to achieve this goal, the Park has engaged in a number of studies aimed at guiding conservation and planning on the Merced River. Among the objectives of this effort is to quantify the impacts of groundwater abstractions on the Merced River and wetlands in Yosemite Valley.

Groundwater pumping in Yosemite Valley provides up to 200 million gallons of water annually to serve the operational needs of the Park. During peak water use in the months of July through September, pumping from three production wells near Yosemite Lodge can reach up to 700,000 gallons per day. At this point, no effort has been made to quantify the impacts of these withdrawals on streamflow in the Merced River and wetland ecosystems in Yosemite Valley or the long-term sustainability of the aquifer.

Purpose

The purpose of this study is to conduct an initial hydrogeologic characterization of a portion of the Yosemite Valley to evaluate the impact of groundwater pumping on streamflow and the water table in meadows during low flow periods (August – October) in 2010.

Project Objectives

The objectives of this project are to (1) review the existing data and reports to better understand the hydrogeology of the Yosemite Valley and (2) to use field monitoring and groundwater modeling to estimate the impact of groundwater abstractions on the low flow hydrology of the Merced River and wetlands adjacent to the Yosemite Lodge.

Project Outcomes

Shallow groundwater was monitored from seven piezometers installed near the confluence of the Merced River and Yosemite Creek. Stage in the Merced River was monitored at two sites and a pool in Yosemite Creek to assess potential stream depletion due to groundwater pumping.

Shallow groundwater levels in piezometers, Yosemite Creek, and the Merced River showed no discernable drawdown or depletion in response to groundwater withdrawals. Results were significantly affected by the pumping protocol which calls for groundwater from the beginning of each pump cycle to be routed onto the land surface. Despite this, a confining layer which separates the water table and stream from the pumped aquifer appears to substantially mitigate the effects of short-term groundwater pumping on shallow groundwater levels and streamflow.

A numerical groundwater model was used to estimate longer term impacts of groundwater pumping on groundwater levels and streamflow in the Merced River. We developed two groundwater models (Model A and Model B) to determine the effect of variability in the permeability of the confining layer on potential impacts. Confining layer hydraulic conductivity varied from 10^{-3} m/day in Model A to 10^{-1} m/day in Model B.

The impact of pumping on stream depletion varies significantly between Model A and Model B. Model A shows a larger (199.5 cm) decrease in groundwater head in the confined aquifer assuming steady-state pumping. Effects of pumping on shallow groundwater heads (<1cm) and streamflow depletion (1.9%) are small. Model B shows that groundwater pumping has significantly greater impact on shallow groundwater heads and streamflow assuming higher confining layer hydraulic conductivity. Confined heads, in this case, declined to a lesser degree (74.56 cm) assuming steady-state pumping. However, shallow groundwater heads drop by up to 32.3 cm and streamflow is depleted by .019 m^3/sec (4.0 %).

Model Limitations

Model results are subject to uncertainty due to the limited time-scale of the data collection period and limited spatial distribution of monitoring sites. Based on the available data, we could not

effectively constrain boundary conditions and aquifer parameters that could impact significantly the model outcomes. The available field data suggests that groundwater pumping likely would not produce significant short-term impacts on streamflow and the water table. Longer term simulations using the model also suggest only modest impact, but this model is highly conceptual and not well-constrained by field data.

Recommendations

This study provides a conceptual model of the hydrogeology in the Yosemite Valley during low-flows used to estimate the potential impact of groundwater pumping on water resources. While this study provides some indication that the effects of groundwater pumping on streams and meadows are limited, the short time allotted for data collection make it difficult to draw definitive conclusions. To more effectively evaluate both the short and long term impacts of groundwater pumping on streams and meadows, we recommend that the Park Service: 1) extend the groundwater and surface water monitoring program near supply wells for a minimum of 1 year 2) install a limited number of additional monitoring wells particularly near model boundaries 3) continue to develop and refine the numerical model to incorporate temporal variability in streamflow, recharge, and evapotranspiration.

INTRODUCTION

Yosemite National Park is one of the best known parks in the United States receiving over 3.7 million visitors annually. Concerns over user impact have resulted in a number of court decisions aimed at more effectively quantifying and mitigating environmental impacts on the Parks natural resources. As part of a 2009 court settlement, the National Park Service has agreed to complete a revised Comprehensive Management Plan for the Merced River to fulfill the requirements of National Environmental Protection Act and Wild and Scenic Act (United States District Court, 2009). In order to achieve this goal, the Park has engaged in a number of studies aimed at guiding conservation and planning on the Merced River. Among the goals of this effort is to quantify the impacts of groundwater withdrawals on the Merced River and wetlands in Yosemite Valley.

Groundwater and surface water are an interconnected and interchangeable resource (Winter, 1999). During periods of low precipitation, the primary source of stream-flow to a basin comes from groundwater. Groundwater fluxes in streambeds, particularly during low flow, play a large role in maintaining the ecological integrity of stream (Brunk and Gonser, 1997; Baxter and Haur, 2000; Hayashi and Rosenberry, 2002). Increasing demands on water resources in recent years have highlighted the importance of recognizing hydrologic continuity and gaining a better understanding of stream aquifer interaction to more effectively manage water resources (Sophocleus, 2002).

Ineffective management of groundwater pumping has been shown to significantly degrade groundwater and surface water resources. Field studies, analytical models, and numerical models have confirmed these effects on both the reach scale and basin scale (Hantush, 1965; Sophocleus; 1995; Nyholm, 2002; Chen and Shu, 2002; Fleckenstien et al. 2004). In some

cases, improper or short-sighted management of groundwater pumping has led to major declines in the flow and ecological integrity in streams and riparian habitats (Glennon, 2002, Zekster et al. 2005).

At this point, no effort has been made to quantify the impacts of groundwater pumping in the Yosemite Valley. This includes reach scale effects in the vicinity of pumping wells, and basin scale effects on the sustainability of the aquifer and groundwater budget. The goals of this study are to estimate the effects of pumping on streamflow and groundwater resources in the Yosemite Valley.

In this report we describe a field monitoring program and conceptual modeling efforts aimed at ascertaining effects of the groundwater pumping on streamflow and wetlands.

HYDROGEOLOGIC SETTING

The Yosemite Valley is a deep, glacially eroded u-shaped valley characterized by high (1000 m) granitic walls located in the central part of the Sierra Nevada. The granite bedrock in the Valley formed during plutonism as a result of tectonic subduction of the Pacific plate beneath the continental crust during the Cretaceous approximately 100 million years ago (mya) (Bateman, 1992). Approximately 30 mya, plate boundaries developed into a predominantly transform fault producing extensional tectonism evident throughout much of the Western United States (Zoback et al., 1981). This process contributed significantly to the westward tipping of the crustal block resulting in uplift throughout the Sierra Nevada range (Huber, 1990). Using measurements of stream incision, Huber (1981) estimated that increased tectonic forcing in the last 10 million years has produced approximately 2000 m uplift in the region. More recently, it has been shown that geomorphic processes as a result of exhumation of the Sierra Nevada may

have also played a role in increased rates of uplift during this period (Small and Anderson, 1995).

Though fluvially derived, the Yosemite Valley was further deepened through scouring, glacial abrasion, and plucking during early, large scale, Sierran glaciations (Matthes, 1930; Huber, 1987). The chronology, extent, and sequence of glaciations in the Sierra Nevada is difficult to quantify, partly because later glaciers obliterate morainal evidence from earlier glaciers (Gibbons et al., 1984). However, geologic evidence suggests that bedrock excavation in the Yosemite was primarily achieved through earlier glaciations ending with the Sherwin which marked the glacial maximum in the Yosemite Valley approximately 750 thousand years ago (kya) (Sharp, 1968; Huber, 1981; Huber, 1987). Though originally thought to have only been deepened to 100 – 200 meters below the current valley bottom (Matthes, 1930), later geophysical studies (Gutenberg et al, 1956) suggest that the depth of the bedrock is up to 600 meters below the current topography in its deepest point. Numerical models have verified that the efficacy of glacial erosion is significant enough under these circumstances to deepen the valley to this extent (Harbor, 1992; MacGregor et al, 2002).

The subsurface sedimentary geology of the Yosemite Valley is largely uncharacterized. However, it is a generally accepted that the bulk of the valley fill is the product deposition of advancing and receding ice sheets during successive periods of glaciations (Matthes 1930; Gutenburg, 1956; Huber; 1987). Evidence of at least Tahoe and later Tioga glaciers is visible as till deposits marking the terminal moraines near Bridalveil Meadow (Matthes, 1930; Huber 1987). Post-Sherwin glaciers lacked the size and efficacy to further erode the bedrock (Huber, 1981). It is more likely that these glaciers rode over glacial fill and lacustrine sediments deposited during and after the Sherwin glaciation (Gutenburg, 1956; Huber, 1987). After the

retreat of Tioga glaciers approximately 16 kya, melt-water streams were impounded behind recessional moraines producing a lake which occupied much of the main portion of the Yosemite Valley (Matthes, 1930; Huber, 1987; Smith and Anderson, 1992). The remainder of the Valley was subsequently filled by silt and fluvial sediments deposited in a prograding delta (Matthes, 1930; Huber, 1987).

Interpretation of sediment logs from 5 borings drilled during 1970-1989 suggests that unconsolidated sedimentary fill in the valley is composed of three hydrofacies (Figure 1). Sediments from boring logs were classified into three units based on estimated hydraulic conductivity (K) values: high K was assigned to intervals containing coarse sand - sand and gravel, medium K was assigned to intervals containing fine – medium sand, and low K was assigned to intervals containing clay – silt. Results from correlating these units somewhat parallel layer geometries reported by Gutenberg et al. (1956) but contradict inferences suggesting that the Valley is predominantly comprised of lacustrine fill. Instead, boring logs indicate that the Yosemite Valley is comprised of at least two aquifer units: an upper, unconfined system and a lower, semi-confined system, with an intervening silt and clay confining layer. It is likely that the confining layer does not extend all the way to the valley walls, and may have windows through it in other portions of the valley where fluvial incision may have occurred after the glacial lake(s) receded.

The Upper Merced River is a tributary to the San Joaquin River which drains into the San Francisco Bay. Its headwater source is a network of tributary streams in an approximately 800 square kilometer watershed. In 1987, the U.S. Congress designated the Merced River as Wild and Scenic, and as a result its flow is predominantly unregulated until it reaches the Central Valley. The climate of Yosemite Valley is characterized by mild winters and long dry summer

months. On average, precipitation peaks in January and reaches a low of 0.17 mm/day during the month of August. During the winter and spring, flow in the Merced River comes predominantly from precipitation and snowmelt. In the summer and fall, streamflow is increasingly dependent on groundwater discharge as overland flow contributions from snowmelt and precipitation decline (Conklin and Liu, 2008).

Groundwater pumping in Yosemite Valley provides up to 200 million gallons of water annually to serve the operational needs of the Park. During peak operation in the months of July through September, pumping from the three production wells near Yosemite Lodge can reach up to 700,000 gallons per day (Water Records 2004-2007). Existing data shows that average daily abstraction from supply wells can reach up to 5% of the daily discharge at Pohono gage. Groundwater is currently withdrawn from 3 supply wells adjacent to the Merced River and Yosemite Creek in the Yosemite Valley (Figure 2). Well #1 is a 15.25 cm diameter well located near the confluence of Yosemite Creek and the Merced River and is screened at depth intervals from 131.5 – 156.3 m below land surface. Well #2 is a 25.5 cm diameter well located adjacent to the eastern bank of Yosemite Creek and is screened on intervals from 152.1 - 213.4 m. Well #4 is a 35.6 cm well located approximately 100 meters west of Well #1 and screened over intervals from 109.7 – 237.7 m.

FIELD MONITORING

Field Methods

Field monitoring of groundwater and surface water in the Yosemite Valley was conducted during the late summer and early fall of 2010. Substantive field operations did not begin until mid August 2010 with shallow groundwater and stream monitoring active by mid

September of 2010. Monitoring of groundwater pumping times and confined aquifer levels began in late September marking the beginning of the analysis period.

Groundwater Monitoring

Shallow groundwater was monitored from seven, 3.175 cm diameter piezometers installed near the confluence of the Merced River and Yosemite Creek (Figure 2). Piezometers were driven by hand to depths ranging from 3.4 to 4.7 m and were screened on a 60 cm interval. Additionally, we monitored one piezometer installed by the USGS in 1970 located 400 m west of Well #4. Records indicate that this piezometer was jetted to a depth 10.85 m but do not include screen information. Water levels were measured using Solinst© Model 3001 pressure transducers that recorded data on a 1 min interval. Manual water level measurements were taken using a steel tape approximately every 2 weeks.

Water levels in the confined aquifer were measured using pressure transducers from Well #2 and Well #4 (Figure 2). Artesian head in these wells prevented manual water levels from being taken using a steel tape. Instead, groundwater heads from these wells were interpreted from the depth of installation of the pressure transducer in the well casing. Daily abstractions from pumping wells were acquired from the Supervisory Control and Data Acquisition (SCADA) system administered by the Yosemite Valley Utilities Dept. Since the SCADA system is not currently programmed to record pumping times, these the pumping intervals were estimated based on observed drawdown in the pumping wells.

Surface Water Monitoring:

Stage in the Merced River and Yosemite Creek was monitored to assess potential stream depletion due to groundwater pumping. Stage was monitored at two sites located upstream and downstream of the abstraction wells and one site in Yosemite Creek (Figure 2). Stage was

measured using Solinst© Model 3001 pressure transducers recording results every 1 min. Manual measurements of stream stage were taken approximately every 2 weeks and during stream discharge measurements. Field observations in late September indicated that discharge in Yosemite Creek was insignificant. However, we were able to record water level fluctuations in a pool adjacent to the stream bank. Stream discharge was estimated on 6 occasions throughout September and early October. Discharge was calculated using a power curve fit to stage and discharge measurements (Figure 8).

Monitoring Results

Water level measurements collected from shallow piezometers indicate that hydraulic head in the unconfined aquifer generally decreases to the west and toward the Merced River (Figure 4). Calculated horizontal hydraulic gradients in the study site range from 0.0015 measured between MW-4A and LM-1, and 0.0039 measured between MW-1A and MW-1B. Water level data from the shallow piezometers varied diurnally by approximately 10 mm: peaking in the early morning and dipping in the early afternoon (Figure 5).

We encountered some error as a result of sedimentation in the piezometers which produced a significant amount of noise in the signal. This effect was particularly evident in MW-2D, MW-1B, and MW-4A. Although we did not discount results from these piezometers, it should be noted that results from these sites are subject to some error. Results from these sites do not significantly affect our analysis of groundwater trends and exhibit similar responses in regard to the effect of pumping.

River stage recorded at gages in the Merced River exhibited a diurnal response (Figure 9). Stream stage in the Merced River peaked in the early morning and declined approximately 5

mm by the early afternoon. Daily variation in water levels recorded in Yosemite Creek was greater (10 mm) and more closely resembled results recorded from piezometers. A greater variance in daily stage in Yosemite Creek than in the Merced River is presumably because of a lack of surface water inflow through Yosemite Creek and because many of these measurements were at low flow conditions and mainly reflect elevation of disconnected pools (i.e., the water table) in the creek.

Effect of Pumping

From July through October 2010, 277,000m^3 of groundwater was pumped from the aquifer in Yosemite Valley. Average daily groundwater withdrawals from supply wells peaked at 2,750 cubic meters per day in August 2010, declining to 1,675 cubic meters per day in October (Figure 3). Extracted amounts were evenly distributed among the three pumping wells in the months of August and October 2010. Well #4 was not appreciably pumped during the month of September due to scheduled maintenance on the well casing and screen. Well #2 was not pumped significantly in the month of July 2010. Pumping rates from July through October of 2010 ranged from 4,830 to 5,026 m^3/day at Well #1, 3521 to 3842 m^3/day at Well #2; and 6198 to 7010 m^3/day at Well #4.

Diurnal fluctuations in stream stage and discharge did not show a strong correlation with well pumping or observed drawdown in the confined aquifer. Diurnal fluctuations in the water table and streamflow are commonly induced by temporal changes in evapotranspiration and plant water use in riparian areas (Loheide et al. 2005; Bond et al. 2005; White, 1932). Though some stage changes correspond with pumping times, stream hydrographs suggest variations are more closely linked to these natural processes (Figure 9). Furthermore, high water demands during the

late summer and early fall prevented us from conducting a pumping test on the scale of days, which would most likely be required to see any appreciable stream depletion. As a result, stream monitoring could not explicitly isolate the effects of pumping on stream stage.

Shallow groundwater levels in piezometers and Yosemite Creek showed no discernable drawdown in response to groundwater withdrawals (Figure 6, Figure 9). Results were significantly affected by the pumping protocol, which calls for groundwater from the beginning of each pump cycle to be routed onto the land surface in order to reduce the turbidity of the drinking water. This "blow-off" water caused a notable spike in the hydrographs in piezometers adjacent to the pumping wells negating the impact of any potential drawdown (Figure 6).

Water levels at MW-2B and MW-2C were not significantly affected by blow-off from Well #1 and Well #4. Consequently, these piezometers were used as a primary source to evaluate any potential impacts of groundwater pumping on shallow water levels. Pumping from Well #4 did not show any appreciable impact on water levels in the piezometers (Figure 7). Effects from pumping at Well #1 were difficult to detect. Water levels at MW-2C show that there could be a small amount of drawdown, but no more than about 5 mm (Figure 7). In both cases it is evident that diurnal variations evapotranspiration and potentially stream stage are the dominant factors controlling shallow groundwater levels on a short time scale.

Heads at the LM-1 piezometer showed some drawdown, particularly in response to pumping at Wells #1 and #4 (Figure 6). Based on boring logs from this site, there is some evidence to suggest that the confining layer thins to some degree near Leidig Meadow (Figure 1). However, it is more likely that drawdown at this site is predominantly influenced by the proximity of this piezometer to the Leidig Meadow Well, which was constructed in a way that may produce a localized hydraulic connection between the two aquifers. It is possible that

pumping influences at this site are localized to the immediate vicinity of the Leidig Meadow Well and do not reflect groundwater trends of the area at large.

From September 28, 2010 to October 3, 2010, groundwater levels after drawdown recovery from deeper aquifer units measured at Well #2 ranged from 1.45 to 1.75 m higher than those measured from nearby piezometers. Limited drawdown (0.55 m) was observed at Well #2 from pumping at Well #4, and at observed at Well #4 from Well #2 (0.05 m). Groundwater pumping at Well #1 produced 1.26 m of drawdown at Well #2 and 3.13 m of drawdown at Well #4.

CONCEPTUAL MODEL

Field monitoring and previous geologic investigations indicate that unconsolidated deposits in the Yosemite Valley can be categorized into at least two aquifers separated vertically by a confining layer of silt and clay (Figure 11). According to boring logs, upper aquifer units are composed primarily of unconsolidated sediments ranging from fine sand to gravel deposited presumably by glacio-fluvial processes during the retreat of Tioga glaciers approximately 16 kya (Matthes, 1930; Huber, 1987). Deeper aquifer units are composed of a variety of unconsolidated materials ranging from boulders to silt and clay. Based on the glacial history of the region, these sediments were probably deposited as glacial outwash, till, and some lacustrine fill during successive glaciations (Sharp, 1968).

In addition to surface recharge from precipitation, groundwater in the Yosemite Valley aquifer system is replenished by lateral subsurface flow from the adjacent fractured rock system (Conklin and Liu, 2008). Although flow rates in the fractured rock portion of the system are considerably lower than in the sedimentary fill, local fracture inflow to the sedimentary fill could

be significant where the fracturing is sufficiently dense and interconnected (Figure 11). Studies from areas with similar geology have shown that flow through bedrock can contribute considerably to the water budget of groundwater basins (Thyne et al., 1999; Wilson and Guan, 2004). In the Yosemite Valley, it has been shown that mountain block recharge to the Yosemite Valley potentially contributes up to 50% of baseflow in the Merced River (Conklin and Liu, 2008).

Lake and stream levels demonstrate that the predominant regional groundwater flow in unconfined aquifer is from the east to the west. Reach-scale field data suggests that groundwater flows towards the Merced River in the study area (Figure 4). Lack of distributed groundwater head data makes it difficult to quantitatively assess the groundwater gradient in the deeper, confined aquifer. However, it is presumed that heads to the east in Tenaya Canyon and near Happy Isles are similar to those of the unconfined aquifer near the extent of the confining layer and decline – becoming artesian (confined or semiconfined) - toward the west.

CONCEPTUAL NUMERICAL MODEL

Numerical modeling can be used to develop a quantitative conceptual model that provides estimates of the water budget for the groundwater system. The code MODFLOW-2000 was used for this analysis because it is exceptionally versatile and offers a variety of modules to simulate a wide range of processes (Harbaugh et al., 2000). Groundwater Vistas was used for pre and post-processing (Rumbaugh and Rumbaugh, 2007).

Field monitoring results do not indicate that groundwater pumping has a significant short term impact on the water table and streamflow. Accordingly, it appears that the confining layer substantially mitigates the effects of groundwater pumping on the water table, and in turn,

streamflow. Additionally, diurnal effects appear to dominate variations in measured head limiting the experimental control we could exercise in discerning any potential effects of abstraction.

Numerical modeling was used to quantitatively estimate the potential effects of groundwater pumping on streamflow. It is assumed that the parameter most likely to affect the variability in of pumping effects is the vertical hydraulic conductivity of the confining layer. Consequently, we developed and calibrated three models that simulate the range of potential effects of vertical *K* variability in the confining layer.

Boundary Conditions

Horizontal boundaries to the flow system were assigned where unconsolidated deposits contact the granite bedrock to the north and south. In the unconfined aquifer and confining beds, this interface was represented as a no-flow boundary. In the confined aquifer, we assigned a head-dependent boundary condition at the bedrock contact simulating recharge from bedrock fracture systems.

To the southwest, the model is bounded by a head-dependent boundary corresponding to the estimated hydraulic head west of Leidig Meadow near the Sentinel Beach Picnic Area. The location of this boundary was selected beyond the area where we would expect to see an appreciable aquifer response from groundwater pumping. The domain is also horizontally bounded to the southeast and northeast by head-dependent boundaries assigned at Happy Isles and Iron Spring in Tenaya Canyon. The location of these boundaries was determined based on the extent of available subsurface data.

The upper boundary of the groundwater model was determined by the land surface. As mentioned before, we know that the hydraulic conductivity of the fractured rock is considerably lower than that of the unconsolidated fill. As a result, the lower boundary of the model was assigned where we assume that the confined aquifer units contact the granite bedrock.

The Merced River and Yosemite Creek incise the upper layer of the model domain. Stream-aquifer interaction between the unconfined aquifer and the Merced River and Yosemite Creek was simulated using the SFR1 package (Prudic et al., 2004).

Discretization

The model domain covers a 5,000 m by 2,760 m portion of Yosemite Valley. The model domain was discretized horizontally into 147 rows and 264 columns. Model cell dimensions near the pumping wells are 10 x 10 meters. For the bulk of the model a coarser – 20 x 20 meter – cell size was used (Figure 12).

The model was initially discretized vertically into 3 layers. The top of layer 1 is the land surface determined by a USGS digital elevation model. The tops of layers 2 and 3 were determined by the top and bottom elevation of the confining layer. Confining layer elevations were estimated from boring logs and correlated laterally from seismic refraction results presented by Gutenberg (1956). The elevation of the bottom of layer 3 and the lower no-flow boundary was estimated exclusively from seismic refraction results of Gutenberg et al. (1956).

The vertical discretization was subsequently refined to 8 layers. Unconfined units that comprise layer 1 were divided into 3 layers. Due to convergence issues attributed to cell drying and rewetting, the bottom elevation of the upper layer was set to 5 meters below the predicted groundwater heads derived from earlier model runs. The remainder was divided equally into two

layers. Confining units (originally layer 2) and confined units (originally layer 3) were divided equally into two and three layers, respectively (Figure 12).

Parameterization

Based on the conceptual model, valley fill was broken up into three primary units to simulate the unconfined aquifer, confining layer, and confined aquifer. Since no field tests were conducted to assess the hydraulic conductivity of the unconfined units, this value was estimated based on the range of reported values for fine sands through gravel ($1.73 \times 10^{-2} – 2.59 \times 10^{3}$ m/day), and refined to 5 - 25 m/day during model calibration (Table 1). Specific yield in the unconfined units was selected on the low end (0.15) of the reported range of 0.10-0.35 for fine sands through gravels (Fetter, 2001).

Based on boring logs, we assume the confining layer is a continuous unit composed primarily of silt and clay which is distributed throughout the majority of the model domain. Interaction between the confined and unconfined aquifer units was shown to be sensitive to the vertical hydraulic conductivity of the confining layer. Consequently, we developed 2 models in order to incorporate the effects of the potential variance in confining layer *K*. The reported hydraulic conductivity of silts ranges from 8.6×10^{-5} to 8.6×10^{-1} m/day (Domenico and Schwartz, 1998). In order to quantify the potential effects of variability in confining layer permeability, we considered vertical *K* values of 1×10^{-3} and 1×10^{-1} m/day hereafter referred to as Model A and Model B. Horizontal confining layer *K* was maintained at 1×10^{-2} m/day in both simulations. The lateral extent of the confining layer is largely unknown though it is assumed to be distributed at variable thickness through the main chamber of the Yosemite

Valley. In Tenaya Canyon and upstream of Happy Isles gage we assumed an isotropic K of 1 x 10^{-1}.

Hydraulic conductivity parameters for the confined layer were approximated based on results from pumping test analysis using the Cooper-Jacob and Theis methods (see Appendix A). Based on these results, we estimated that aquifer transmissivity in the vicinity of the pumping wells ranges from 507 to 1160 m^2/day ($K \approx 5$ to 20 m/day) and storativity ranges from 3.54 x 10^{-4} to 6.56 x 10^{-3} ($S_s \approx 4$ x 10^{-6} to 2 x 10^{-5}). A more refined estimation of aquifer properties was developed during model calibration based observed drawdown results to a value of 5 m/day. Due to a limited subsurface geologic data in the valley, we assumed a simplified and constant distribution of hydraulic conductivity and specific storage to be constant in all confined units.

Distributed recharge from direct precipitation in the Yosemite Valley during low flows is very small. The average daily precipitation during the month of August in the Yosemite Valley over the last 8 years was 0.17 mm/day. The total precipitation during the months of July – September of 2010 was 1.22 mm. Consequently, we did not simulate any distributed recharge over the model domain in order to reflect recharge conditions in September, 2010.

The component of lateral subsurface flow attributed to fracture flow from the valley walls was simulated using a combination of specified fluxes and head-dependent boundary conditions. Groundwater flow from fractures into unconfined units was simulated using a specified flux along cells adjacent to the no flow boundary in layer 1 (Figure 12). Fluxes ranged from 1,180 m^3/day in Model A to 5,900 m^3/day in Model B (Table 1). Bedrock fracture flux into the confined aquifer was simulated using a head-dependent boundary condition (Figure 12). Based on the elevation of the valley walls, we assumed groundwater heads in fractures to be significantly higher than those in the sedimentary units in the valley bottom. Heads were

initially assigned as 1250 m, but due to model instability were set to 1240 m in the eastern portion of the domain, 1220 m in the central portion, and 1210 m in the western portion. Conductance of the general head boundaries ranges from 2 x 10^{-1} m^2/day in Model A and 2 x 10^{-1} m^2/day in Model B (Table 1).

Evapotranspiration was simulated using the Evapotranspiration Package in MODFLOW 2000 (Harbaugh et al., 2000). Reference evapotranspiration was estimated from a state-wide zone map and was assumed to be 6.7 mm/day (CIMIS, 1999). Due to a lack of data pertaining to crop coefficients (*Kc*) for vegetation types in the Yosemite Valley, we initially assumed a *Kc* of 1 for all vegetated areas and a *Kc* of 0 for bedrock, talus, and urbanized areas. *Kc* was subsequently adjusted based on the reported vegetation density in order to more accurately approximate potential evapotranspiration. Rooting depths were roughly estimated based on a vegetation type map of the Yosemite National Park (ESRI, 2007). Rooting depths for each vegetation zone were roughly approximated (Table 2) from values reported from the literature (Canadell et al. 1996).

Stream-aquifer interactions were simulated using the SFR1 package (Prudic et al. 2004). The Merced River was broken up into 14 stream segments with one additional segment to simulate potential interactions in Yosemite Creek (Figure 12). The SFR1 package assumes a constant slope in any stream segment (Prudic et al. 2004). As a result, stream segments were initially delineated based on changes in the slope of the river channel assessed through a LIDAR elevation dataset. Reaches were additionally broken up at the confluence of the Merced River and Yosemite Creek and at the two stream gage locations. Stream boundaries were not simulated upstream of the USGS gage at Happy Isles and Tenaya Creek due to an absence of actual or estimated streamflow data in these areas.

Flow entering the first segment of the Merced River at Happy Isles was estimated to be 2.23 x 10^4 m^3/day based on observed streamflow at the USGS gage on September 30th. The USGS does not currently maintain a gage at Tenaya Creek. As a result, flow entering Tenaya Creek was estimated based on the relationship between historical flows at the USGS gage at Happy Isles and Tenaya Creek from the last 10 years of available data from both sites (Figure 13). The relationships between flows at the two sites is not strong (R^2 = .39), therefore the estimated flow at Tenaya Creek (3.75 m^3/day), however provides a rough approximation of flow entering this segment. During the late summer and fall, streamflow in Yosemite Creek is negligible and was not simulated.

Due to a lack of data, particularly in upper stream reaches, we were forced to make a number of simplifications to stream boundary parameters. Lateral stream geometry was simplified and assigned as a wide rectangular channel. Boundary widths were maintained constant in all reaches of the Merced River up-stream of the Tenaya Creek confluence (5 m), in Tenaya Creek (3 m), downstream of the Tenaya Creek confluence (10 m), and in Yosemite Creek (3 m). We assumed a streambed thickness of 1 meter for all stream reaches. Hydraulic conductivity of the streambed was assigned as 10 m/day based on reported results for sand and gravel streambeds (Calver, 2001). The reported value for Mannings roughness coefficient of 0.065 at Happy Isles was used in all stream reaches (Limineros, 1970).

Calibration Parameters

Model parameters were estimated by fitting model results to three datasets including drawdown and recovery results recorded from pressure transducers in Well #2 and Well #4,

groundwater heads on September 30th, 2010, and calculated streamflow at MR_West and MR_East.

Due to continual groundwater pumping during the study period, we encountered some difficulty in developing a baseline model calibration. Heads, particularly in confined units near the pumping wells, are affected by short-term (minutes to hours) localized drawdown due to groundwater pumping, and longer-term (monthly to yearly) regional drawdown that does not completely recover during the short periods when the aquifer is not pumped. To simulate long term, regional drawdown effects of groundwater pumping, we developed a steady-state model assuming average total daily groundwater withdrawals. To limit the impact of short term drawdown effects on calibration targets, we selected measured groundwater heads and stream-flow after 12 hours of groundwater recovery on September 30th 2010. Recovery was reproduced in a 12-hour transient simulation with an initial time-step of 1.66 minutes and a time-step multiplier of √2.

A transient simulation was conducted in order to fit simulated results to observed drawdown and recovery from 4:40 PM on October 2 to 4:55 PM on October 3, 2010. This period was selected because it provided a consistent, uninterrupted dataset with pumping from Well #1. In order to simulate regionally lowered baseline groundwater levels for the simulation we developed a steady-state simulation assuming constant pumping from Well #1 at 2500 m^3/day allowing for 12 hours of recovery (see above). Pumping was simulated at a rate of 5,000 m^3/day based on records from the SCADA system at Well #1 for 590 minutes followed by 865 minutes of recovery. We assumed an initial time-step of 1.36 minutes for pumping and 1.99 minutes for recovery. Subsequent time-steps used in both drawdown and recovery were increased as a geometric progression of ratio √2 of the previous time-step.

Results

Simulated results correlate well with the observed head on September 30, 2010. The absolute residual mean error between simulated and observed heads ranged from 9 cm in Model B and 10 cm for Model A (Table 3). Model A predicts slightly lower (-10 cm) mean groundwater heads than observed in shallow piezometers. Model B more accurately simulates shallow groundwater heads in this area with a residual mean error of 2 cm. Residual heads calculated at the piezometer located near the Leidig Meadow Well (LM-1) are negative in both Model A (-37 cm) and Model B (-20 cm). Both models were able to accurately simulate measured vertical gradients between the confined aquifer and the water table despite differences in confining layer vertical *K* (Table 3).

Models A and B deviate slightly in their capacity to accurately simulate observed streamflow at gaged sites on the Merced River. Model A effectively simulates measured flow at both the gages with errors ranging from 3.28% at MR_East and 3.47% at MR_West (Table 4). Additionally, Model A simulates the observed stream gain between the two gage sites to within .001 m^3/sec (14.29%). Model B significantly overestimates streamflow at both stream gages. At the MR_East site simulated flow is 0.063 m^3/sec (15.42%) higher than observed.

Simulated results approximate the observed drawdown in wells reasonably well for a first-cut conceptual model. Field results demonstrate that maximum observed drawdown was 0.95 m at Well #2 and 3.21 m at Well #4. Simulated results indicate that the model overestimates the maximum drawdown at Well #2 by 0.30 m and underestimated results at Well #4 by 1.77 m (Figure 15). Improved accuracy at each monitoring well was achieved by varying the hydraulic conductivity and storage coefficient of the confined aquifer between Well #1 and the observation points. However, due limited subsurface geologic data in the Yosemite Valley,

we assumed a constant hydraulic conductivity for confined units in the model domain. Consequently, the predicted results reflect an effort to define a conductivity value that could be applicable on the scale of the entire basin and do not replicate smaller-scale heterogeneity observed between the pumping wells. This was achieved by simulating mid-range quantity of drawdown at the two observation sites. Simulated drawdown was not significantly impacted by varying the vertical *K* of the confining layer.

Impacts of Pumping

The numerical model is used to quantify hydrologic fluxes in the Yosemite Valley and estimate the impact of pumping from water supply wells on groundwater resources and streamflow in the Merced River. The model incorporates the major hydrologic processes including groundwater recharge, discharge, evapotranspiration, and stream-aquifer interactions based on the conceptual model of the Valley. Due to the limited time-scale available for data acquisition, the model focuses solely on the water budget during low flows in the late summer and early fall. However, with further data collection, the model could be expanded to more comprehensively assess seasonal variations in the groundwater budget and the long-term aquifer sustainability.

The water budget of the Yosemite Valley was initially evaluated in a steady-state simulation assuming constant pumping. During September and August, average daily groundwater abstraction ranged from 1,963 to 2,750 m^3/day. Groundwater pumping from the three supply wells was simulated as a 2,500 m^3/day steady-state boundary condition from Well #1 to provide a simplified representation of typical groundwater withdrawals from the aquifer during the peak season in Yosemite Valley. Boundary conditions representing groundwater

recharge and discharge processes, evapotranspiration, and stream-aquifer interactions were obtained from the calibrated models (Model A/Model B).

In order to estimate the potential impacts of groundwater pumping on groundwater fluxes, heads, and stream-aquifer interactions, we conducted a steady-state simulation assuming pristine conditions (no groundwater pumping). Initial modeling efforts indicated a significant decrease in groundwater fluxes from head-dependent boundaries simulating lateral recharge when pumping was removed from the system. In order to address this issue, fluxes from head dependent recharge boundaries in the pumping simulation were converted into specified flux boundaries in pristine simulations. In this manner, recharge remained constant between pumping and pristine modeling simulations.

Results show a similar total amount of groundwater flux simulated through the model domain in Model A (19,075 m^3/day) and Model B (20,175 m^3/day) assuming steady-state groundwater pumping (Figure 16). However, boundary specific influxes varied considerably between the models. Model A shows greater lateral subsurface flow from mountain-block groundwater in unconfined units (5,900 m^3/day) as compared to Model B (1,180 m^3/day). Conversely, simulated results from Model B show much greater amount of mountain-block recharge in confined units (14,144 m^3/day) than Model A (3,634 m^3/day). During model calibration, we significantly manipulate the dynamics of mountain block recharge in order to effectively maintain observed vertical hydraulic gradients between the confined and unconfined aquifer units. This can be attributed to greater amounts of vertical leakage through the confining layer assuming higher vertical confining layer *K* (Table 5). Additionally, the two realizations deviate significantly in the proportion of total groundwater recharge attributed to mountain block recharge. Model A receives 54% of inflow from fracture flow in bedrock units while Model B

receives 76%. The lateral subsurface flow component of groundwater inflow from the upstream and downstream sedimentary regions to the models also varied considerably between Model A (8,041 m^3/day) and Model B (4,780 m^3/day). Stream losses from the Merced River also contributed significantly (1,500 m^3/day) to the water budget in Model A.

Both cases indicate that groundwater withdrawals from supply wells are not insignificant in the hydrologic budget of the Yosemite Valley. The majority of groundwater losses in the basin occur through aquifer interaction with the Merced River. Net stream gain in Model A accounted for 9,222 m^3/day (52.4%) flux from the groundwater supply and 12,602 m^3/day (62.7%) flux in Model B (Figure 16). Results show that water withdrawals from pumping wells account for from 13.1% of the total water budget in Model A and 12.4% in Model B. The amount lost to evapotranspiration in Model A (1,392 m^3/day) and Model B (1,789 m^3/day) represents a significantly lower loss (Figure 16). Lateral subsurface flow from the western boundary of the model domain are somewhat consistent between Model A (4,453 m^3/day) and Model B (3,213 m^3/day).

The simulation assuming no groundwater abstractions approximates the potential impact of groundwater pumping on the hydrologic budget, water table, and streamflow in the Merced River. Both models predict significant changes in lateral subsurface outflow and stream gain (Figure 17). By using specified fluxes to simulate aquifer recharge to the model domain, we were able to isolate the effects of groundwater pumping to parameters that would most likely be affected. Model A shows a significant increase in lateral subsurface flow out of the domain (1,781 m^3/day) and a minor decrease (684 m^3/day; 0.279 cfs) in streamflow. Conversely, Model B shows a greater increase in stream gain (1616 m^3/day; .661 cfs) and lesser increase in lateral

subsurface flow out of the model domain (743 m^3/day). Model B also shows a slightly (141 m^3/day) greater evapotranspiration which is relatively negligible (36 m^3/day) in Model A.

Impacts of groundwater pumping on groundwater heads and stream depletion vary significantly between Model A and Model B. Model A shows a larger (199.5 cm) decrease in groundwater head in the confined aquifer assuming steady-state pumping. Effects of pumping on shallow groundwater heads (<1cm) and streamflow depletion (1.9%) are small (Table 6; Figure 14). Model B indicates that groundwater pumping can potentially have a more significant impact on shallow groundwater heads and streamflow assuming higher confining layer *K*. Confined heads, in this case, declined to a lesser degree (74.56 cm) assuming steady-state pumping. However, shallow groundwater heads drop by up to 32.3 cm and streamflow is depleted by .019 m^3/sec (4.0%) (Table 6; Figure 14).

MODEL LIMITATIONS

Numerical groundwater models are created based on simplified assumptions used to replicate complex natural systems. Consequently, results are generally subject to errors and limitations due to conceptual misunderstandings of the hydrologic system, uncertainties and shortfalls in estimating aquifer properties and boundary conditions, and spatial and temporal inadequacies in calibration parameters. At this time the groundwater model provides a conceptual representation of the principle hydrologic processes in the Yosemite Valley based on the existing dataset. Deficiencies in these data significantly limit our ability to validate the key parameters and boundary conditions or effectively develop a groundwater model with strong predictive capacity.

Model results are subject to uncertainty due to the limited time-scale of the data collection period and limited spatial distribution of monitoring sites. Based on the available data, we could not effectively constrain boundary conditions and aquifer parameters that could impact significantly the model outcomes. The available field data suggests that groundwater pumping likely would not produce significant short-term impacts on streamflow and the water table. Longer term simulations using the model also suggest only modest impact, but this model is highly conceptual and not well-constrained by field data.

SUMMARY AND CONCLUSIONS

Field monitoring did not conclusively reveal the effect of groundwater pumping on streamflow and shallow groundwater heads. Blow-off from supply wells significantly affected results from near-well piezometers (Figure 6) preventing us from isolating the drawdown effects from pumping. Results from stream gages and piezometers further from the pumping source are impacted by diurnal variations in head which makes potential drawdown effects from groundwater pumping difficult to discern (Figure 7). Current field data suggests that it is likely that short term (hours to days) impacts of pumping on shallow groundwater heads and streamflow are small. In order to try and more definitively quantify the response of pumping on the water table and streamflow, an effort needs to be made to run a significantly longer pumping test and route the blow-off water downstream of the area likely to be affected by the cone of depression. It would also be prudent to investigate how the wells can be run in a way that avoids having to blow-off water from the wells at commencement of pumping.

Numerical modeling shows that despite the variability in the effects of steady-state groundwater pumping on groundwater heads and streamflow. Both simulations suggest that it is not likely that groundwater pumping has an appreciable effect on streamflow. Model B, which simulates a greater hydrologic connection between deep and shallow aquifer units, predicts significantly more groundwater interaction between the deeper aquifer units and the water table. However, the effects of pumping propagated to the Merced River only results in a (4.0%) decline in streamflow at the western boundary of the model domain. Assuming a vertical K of 1×10^{-3} m/day, impacts are significantly less pronounced; producing only a (1.9%) depletion in streamflow.

RECOMMENDATIONS

This study provides a conceptual model of the hydrogeology in the Yosemite Valley during low-flows used to estimate the potential impact of groundwater pumping on water resources. While this study suggests that the effects of groundwater pumping on streams and meadows are limited, the short time allotted for data collection make it difficult to draw definitive conclusions. To more effectively evaluate both the short and long term impacts of groundwater pumping on streams and meadows, we recommend that the Park Service: 1) extend the groundwater and surface water monitoring program near supply wells for a minimum of 1 year 2) install a limited number of additional monitoring wells particularly near model boundaries 3) continue to develop and refine the numerical model to incorporate temporal variability in streamflow, recharge, and evapotranspiration.

REFERENCES CITED

Bateman, P.C. 1992. Plutonism in the central part of the Sierra Nevada batholith, California. U.S. Geological Survey Professional Paper 1483. USGS, Washington D.C.

Baxter C.V., and R.F. Hauer. 2000. Geomorphology, hyporheic exchange, and selection of spawning habitat by bull trout (*Salvelinus confluentus)* 57, no.1: 1470-1481.

Bond, B.J., J.A. Jones, G. Moore, N. Phillips, D. Post, J.J. McDonald. 2002. The zone of vegetation influence of baseflow revealed by diel patterns of streamflow and vegetation water use in a headwater basin. *Hydrologic Processes* 16, no. 1: 1671-1677.

Brunk, M., and T. Gonser. 1997. The ecological significance of exchange processes between rivers and groundwater. *Freshwater Biology* 37, no. 1: 1-33.

Calver, A. River-bed permeabilities: Information from pooled data. *Groundwater* 39, no. 4, 546-553.

Canadell, J., R.B. Jackson, J.R. Ehleringer, H.A. Mooney, O.E. Sala, and E.D. Schulze. Maximum rooting depth of vegetation types at the global scale. *Oecologia* 108, no. 1: 583-595.

Chen, X., and L. Shu. 2002. Stream-aquifer interactions: Evaluation of depletion volume and residual effects from groundwater pumping. *Groundwater* 40, no. 3: 284-290.

Conklin, M.H., and F. Lui. 2008. *Groundwater Contributions to Baseflow in the Merced River: Processes, Flow Paths, and Residence Times.* California Energy Commission, PIER Energy-Related Environmental Research Program. CEC-500-2007-116.

Cooper, H.H., and C.E. Jacob. 1946. A generalized graphical method for evaluating formation constants and summarizing well field history. *Transactions of the American Geophysical Union* 27, no.1: 526-534.

D.L. Peck. 2002. Geologic map of the Yosemite Quadrangle, central Sierra Nevada, California. U.S. Geologic Investigations Series Report I-2751. USGS, Reston, VA.

Domenico, P.A., and F.W. Schwartz. 1998. *Physical and Chemical Hydrogeology*. New York: John Wiley.

Environmental Systems Research Institute, Inc. 2007. Yosemite National Park and environs: National vegetation classification standard.

Fetter, C.W. 2004. *Applied Hydrogeology: Fourth Edition.* Upper Saddle River, NJ: Prentice-Hall, Inc.

Fleckenstein, J., R. Niswonger, and G.E. Fogg. 2006. River-aquifer interactions, geologic heterogeneity and low-flow management. *Ground Water* 44, no. 6: 837-852.

Friends of the Yosemite Valley et al. v. Salazar. CV-F-00-6191. 4. U.S. Dis. Ct. 2009.

Gibbons, A.B., J.D. Megeath, and K.L. Pierce. 1984. Probability of moraine survival in a succession of glacial advances. *Geology* 12, no. 1: 327-330.

Glennon, R.J. 2002. *Water Follies, Groundwater Pumping and the Fate of America's Fresh Water.* Washington D.C.: Island Press.

Gutenberg, B., J.P. Buwalda , and R.P. Sharp. 1956. Seismic explorations on the floor of Yosemite Valley, California. *Bulletin of the Geological Society of America* 67, no.1: 1051-1078.

Hantush, M.S. 1965. Wells near streams with semipervious beds. *Journal of Geophysical Reaearch* 70, no. 12: 2829-2838.

Harbaugh, A.W., E.R. Banta, M.C. Hill, and M.G. McDonald. 2000. MODFLOW-2000, the U.S. Geological Survey modular ground-water model – User guide to modularization concepts and the ground-water flow process. U.S. Geological Survey Open-File Report 00-92. USGS, Reston, VA.

Harbor, J.M. 1995. Development of glacial valley cross sections under conditions of spatially variable resistance to erosion. *Geomorphology* 14, no. 1: 99-107.

Hayashi, M., and D.O. Rosenberry. 2002. Effects of ground water exchange on the hydrology and ecology of surface water. *Groundwater* 40, no. 3: 309-316.

Huber, N.K. 1981. Amount and timing of late Cenezoic uplift and tilt of the central Sierra Nevada, California – Evidence from the upper San Juaquin River basin. U.S. Geological Survey Professional Paper 1197. USGS, Washington D.C.

Huber, N.K. 1987. The geologic story of Yosemite National Park. U.S. Geological Survey Bulletin 1595. USGS, Washington D.C.

Huber, N.K. 1990. The late Cenezoic evolution of the Tuolomne River, central Sierra Nevada, California. *Geological Society of America Bulletin* 102, no. 1: 102-115.

Jones, D.W., R.L. Snyder, S. Eching, and H.G. MacPherson. 1999. Reference evapotranspiration. Department of Water Resources, Sacramento, CA.

Kistler, R.C. 1973. Geologic Map of the Hetch Hetchy Reservoir Quadrangle, Yosemite National Park, California. Geologic Quadrangle Map. U. S. Geological Survey Report GQ-1112. USGS, Reston, VA

Limerinos, J.T. 1970. Determination of Manning Roughness Coefficient from measured bed roughness in natural channels. U.S. Geological Survey Water-Supply Paper 1898-B. USGS, Washington D.C.

Loheide, S.P., J.J. Butler, and S.M. Gorelick. 2005. Estimation of groundwater consumption by phreatophytes using diurnal water table fluctuations: a saturated – unsaturated flow assessment. *Water Resources Research* 41, no. 1: 1-14.

MacGregor, K.R., R.S Anderson, S.P. Anderson, and E.D. Waddington. 2002. Numerical simulations of glacial-valley longitudinal profile elevation. *Geology* 28, no. 1: 1031-1034.

Matthes, F.E. 1930. Geologic history of Yosemite Valley. U.S. Geological Survey Professional Paper 160. USGS, Washington D.C.

Prudic, D.E., L.F. Konikow, and E.R. Banta. A new streamflow-routing (SFR1) package to simulate stream-aquifer interaction with MODFLOW-2000. U.S. Geological Survey Open-File Report 2004-1042. USGS, Carson City, NV.

Rantz, S.E., et al, 1982. Measurement and Computation of Streamflow. U. S. Geological Survey Water-Supply Paper 2175. USGS, Reston, VA.

Rumbaugh, J.O., and D.B. Rumbaugh. 2007. *Guide to using Groundwater Vistas*. Reynolds, PA: Environmental Simulations Inc.

Sharp, R.P. Sherwin Till – Bishop Tuff geological relationships, Sierra Nevada, California. 1968. *Geologica Society of America Bulletin* 79, no.1: 351-364.

Small, E.E., and R.S. Anderson. 1995. Geomorphically driven late Cenezoic rock uplift in the Sierra Nevada, California. *Science* 270, no.1: 277-280.

Smith, S.J., and S. Anderson. Late Wisconsin paleoecological record from Swamp Lake, Yosemite National Park, California. *Quaternary Research* 38, no 1: 91-102.

Sophocleous, M. 2002. Interactions between groundwater and surface water: The state of the science. *Hydrogeology Journal* 10, no. 1: 52-67.

Thyne, G.D., J.M. Gillespie, and J.R. Ostdick. Evidence for interbasin flow through bedrock in the southeastern Sierra Nevada. *Geological Society of America Bulletin* 111, no. 11: 1600-1616.

White, W.N. A method of estimating ground-water supplies based on discharge from plants and evaporation from soil: Results of investigations in Escalante, Utah. U.S. Geological Survery Water-Supply Paper 659-A. USGS, Washington D.C.

Wilson, J.L., and H. Guan. Mountain block hydrology and mountain front recharge. *Groundwater Recharge in a Desert Environment.* Washington D.C.: AGU.

Winter, T.C. 1999. Relation of streams, lakes, and wetlands to groundwater flow. *Hydrogeology Journal* 7, no. 1: 28-45.

Zektser, S., H.A Loaiciga, and J.T. Wolf. 2005. Environmental impacts of groundwater overdraft: Selected case studies in the southwestern United States. *Environmental Geology* 47, no. 1: 396-404.

Zoback, M.L., R.E. Anderson, and G.A. Thompson. 1981. Cenezoic evolution of the state of stress and style of tectonism of the Basin and Range province of the western United States. *Philosophic Transactions of the Royal Society A* 300, no. 1: 407-434.

FIGURE CAPTIONS

Figure 1. Subsurface hydrogeologic interpretation of the Yosemite Valley based on existing well borings.

Figure 2. Site map indicating locations of supply wells, piezometers, and stream gages.

Figure 3. Average daily groundwater withdrawal from Yosemite Valley Pumping Wells July – October, 2010.

Figure 4. Interpreted shallow groundwater heads on September 30th 2010.

Figure 5. Diurnal fluxes observed in near well piezometers September 28th – October 3rd 2010.

Figure 6. Observed effects of groundwater pumping from Well #1 (red), Well #2 (blue), and Well #4 (green) at near-well piezometers**.**

Figure 7. Observed drawdown in response to pumping at Well #1 (top) and Well #4 (bottom).

Figure 8. Stream stage and discharge rating curves from sites MR_East and MR_West.

Figure 9. Observed stage in the Merced River and Yosemite Creek September 28th – October 3rd 2010.

Figure 10. Observed discharge at MR_East and MR_West September 28th – October 3rd 2010.

Figure 11. Conceptual hydrogeologic model of the Yosemite Valley illustrating aquifer units, confining layers, and groundwater flow dynamics.

Figure 12. Model domain, discretization, and boundary conditions.

Figure 13. Relationship between low-flow discharge at the USGS gage at Happy Isles and Tenaya Creek (1947 – 1957).

Figure 14. Observed vs. simulated stream discharge from Model A and Model B under steady-state pumping and pristine conditions.

Figure 15. Observed vs. simulated drawdown at Well #2 and Well #4.

Figure 16. Calculated groundwater fluxes from model boundaries from Model A and Model B assuming steady-state groundwater pumping.

Figure 17. Predicted changes in groundwater fluxes given pristine conditions.

TABLES

Table 1. Model assumptions used in Model A and B

Model	**Model A**	**Model B**
Vertical Hydraulic Conductivity (m/day)	1×10^{-3}	1×10^{-1}
Boundary Elevation (m)	1199.3	1201.5
Boundary Conductance (m2/day)	2×10^{-1}	8×10^{-1}
Recharge (m3/day)	5900	1180
Unconfined Hydraulic Conductivity (m/day)	5 - 25	5

Table 2. Estimated rooting depths of vegetation in the Yosemite Valley

Vegetation Type	**Rooting Depth (m)**
Meadow Grass	2.5
Conifer	3.5
Deciduous	4
Oak	7.5
Willow	2.2
Mixed Oak and Pine	5

Table 3. Observed vs. simulated groundwater heads, residual errors, and absolute residual mean error yielded from Model A and B (confined heads in italics).

Monotoring Well	**Observed Head (m)**	**Simulated Head (m)**		**Residual Error (m)**	
		Model A	***Model B***	***Model A***	***Model B***
MW-1A	1203.64	1203.61	1203.70	-0.03	0.06
MW-1B	1203.76	1203.60	1203.68	-0.16	-0.08
MW-2A	1203.85	1203.76	1203.94	-0.09	0.09
MW-2B	1203.84	1203.78	1203.95	-0.06	0.11
MW-2C	1203.80	1203.75	1203.88	-0.05	0.08
MW-4A	1203.45	1203.48	1203.52	0.03	0.07
LM-1	1202.94	1202.57	1202.74	-0.37	-0.20
Well #2	1205.34	1205.33	1205.40	-0.01	0.06
Absolute Residual Mean Error (m)				0.10	0.09

Table 4. Observed vs. simulated stream discharge

	Observed (m^3/sec)	Simulated Stream Discharge m3/sec		Percent Error	
		Model A	***Model B***	***Model A***	***Model B***
MR-East	0.402	0.3888	0.464	-3.28	15.42
MR-West	0.409	0.3948	0.464	-3.47	13.45
Gain	0.007	0.006	0.004	-14.29	-42.86

Table 5. Vertical groundwater fluxes through the confining layer.

Vertical Flux (m^3/day) Pumping		Vertical Flux (m^3/day) Pristine		Δ Flux (m^3/day)	
Model A	***Model B***	***Model A***	***Model B***	***Model A***	***Model B***
149	8162	263	9228	114	1066

Table 6. Increase in calculated groundwater head assuming no groundwater abstractions.

Monitoring Well	Change in Groundwater Head (cm)	
	Model A	***Model B***
MW-1A	.55	27.25
MW-1B	.48	22.02
MW-2A	.54	24.73
MW-2B	.55	24.72
MW-2C	.44	16.92
MW-4A	.66	32.35
LM-1	.73	23.13
Well #2	199.54	74.57

FIGURES

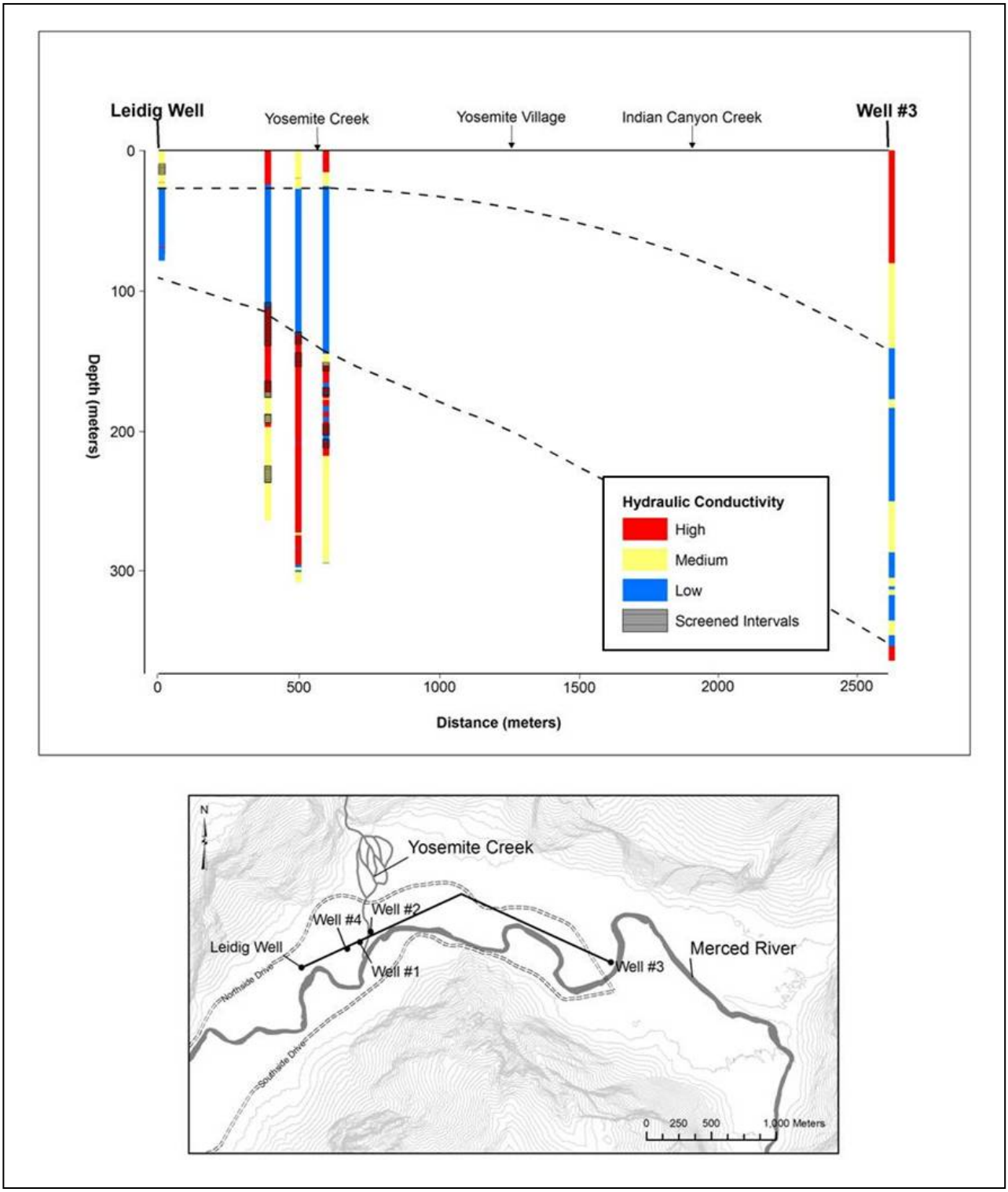

Figure 1

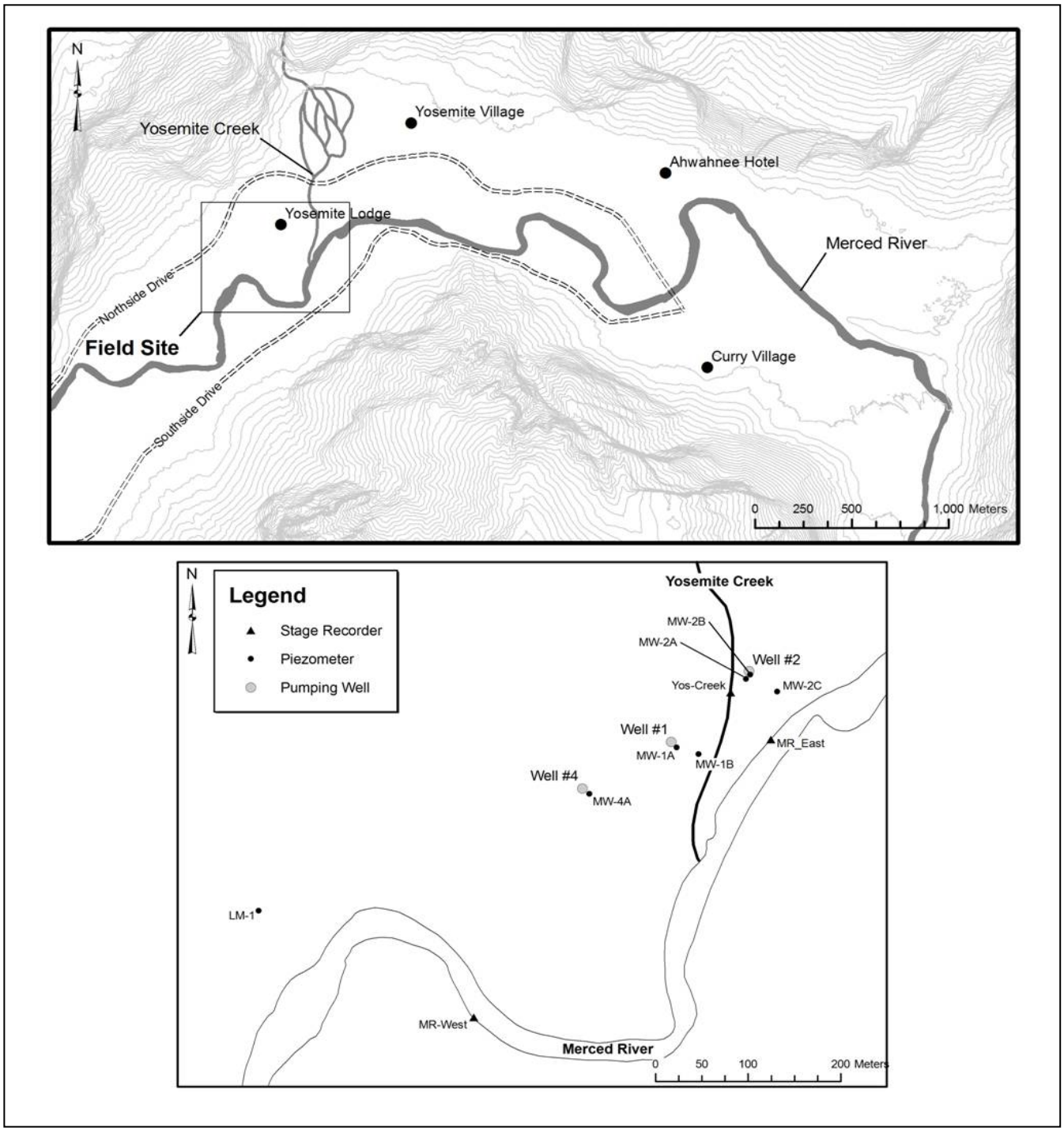
N
Yosemite Creek
Yosemite Village
Ahwahnee Hotel
Yosemite Lodge
Merced River
Northside Drive
Field Site
Curry Village
Southside Drive
0 250 500 1,000 Meters
N
Legend
Stage Recorder
Piezometer
Pumping Well
Yosemite Creek
MW-2B
MW-2A
Well #2
Yos-Creek
MW-2C
Well #1
MW-1A
MW-1B
MR_East
Well #4
MW-4A
LM-1
MR-West
Merced River
0 50 100 200 Meters

Figure 2

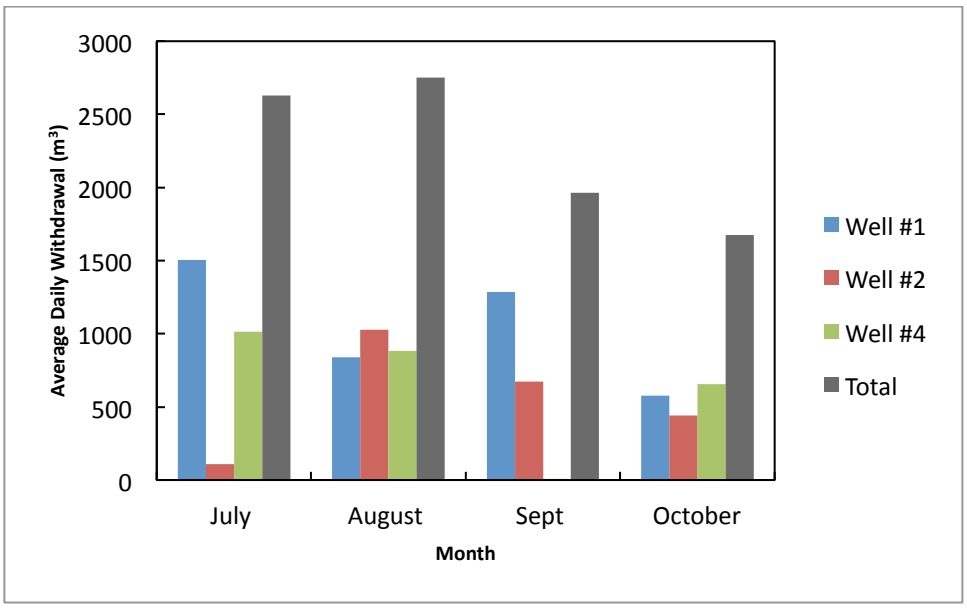

Figure 3

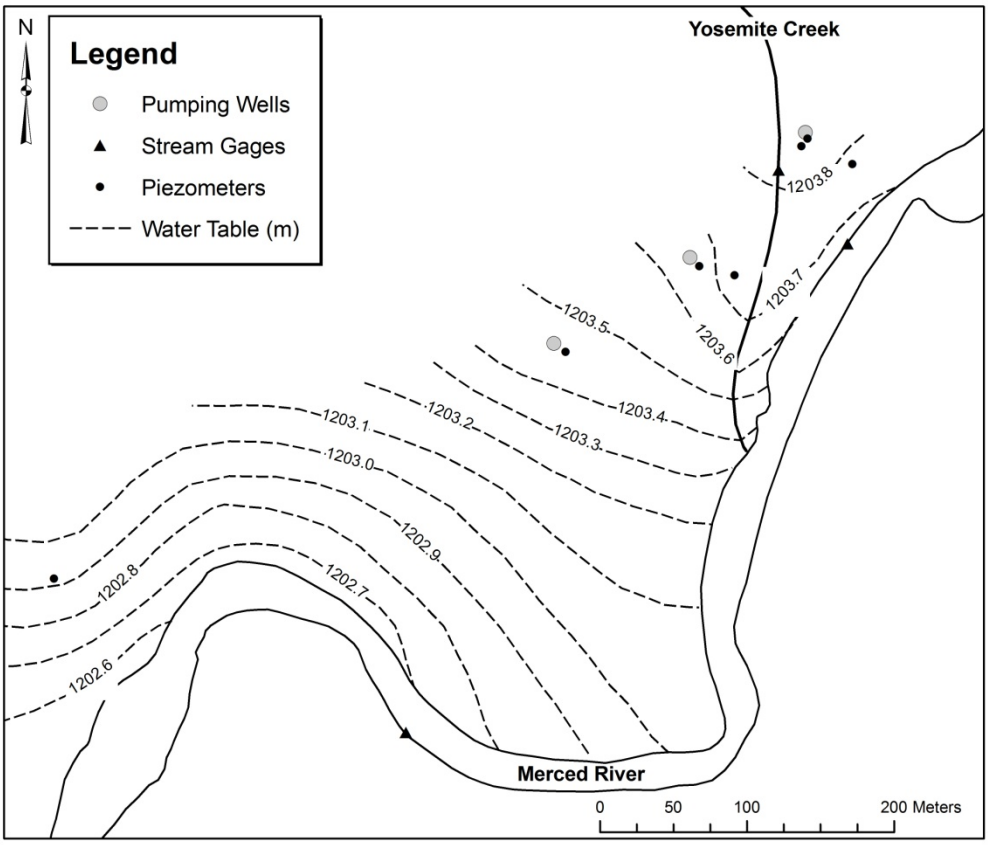

Figure 4

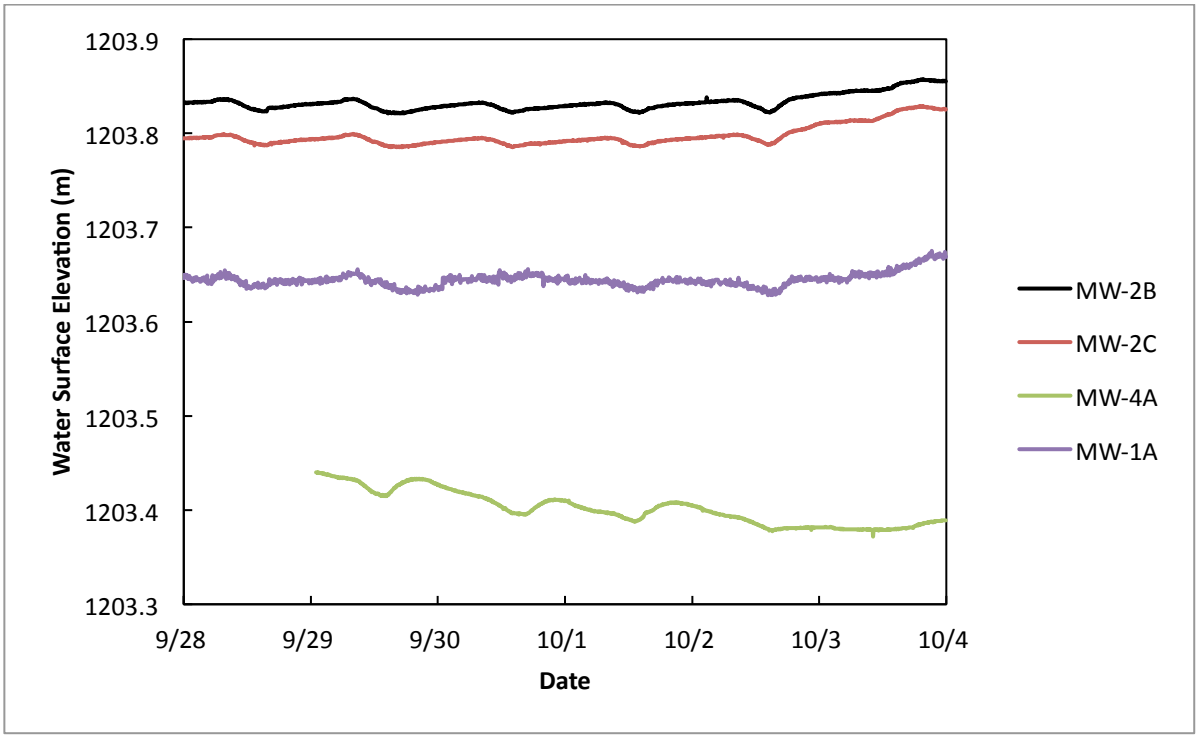

Figure 5

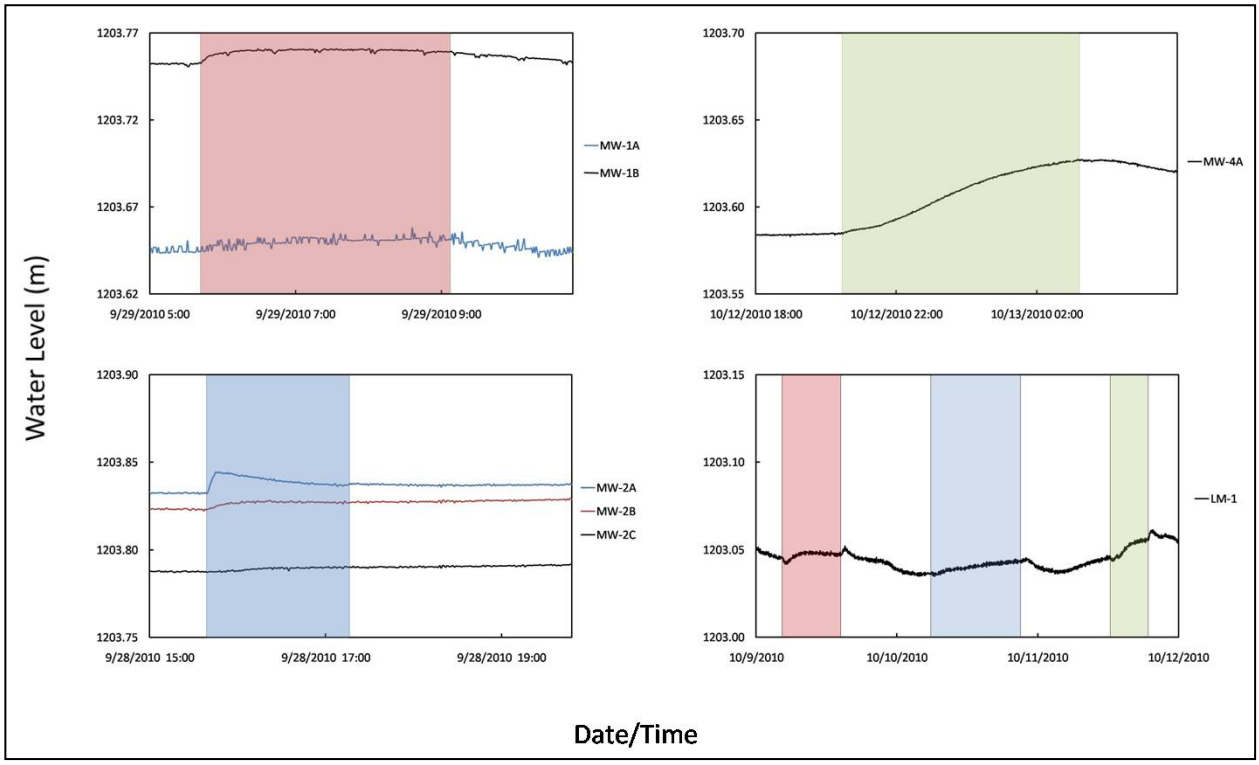

Figure 6

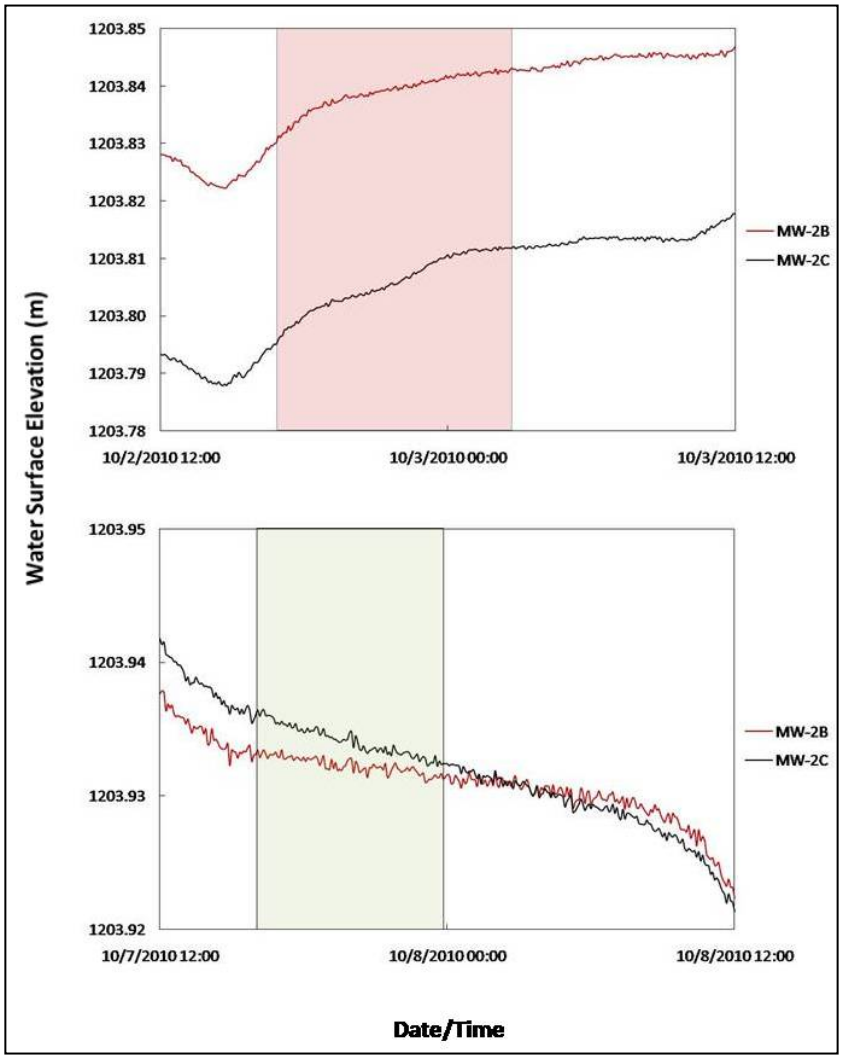
Water Surface Elevation (m)
1203.85
1203.84
1203.83
1203.82
1203.81
1203.80
1203.79
1203.78
10/2/2010 12:00
10/3/2010 00:00
10/3/2010 12:00
MW-2B
MW-2C
1203.95
1203.94
1203.93
1203.92
10/7/2010 12:00
10/8/2010 00:00
10/8/2010 12:00
MW-2B
MW-2C
Date/Time

Figure 7

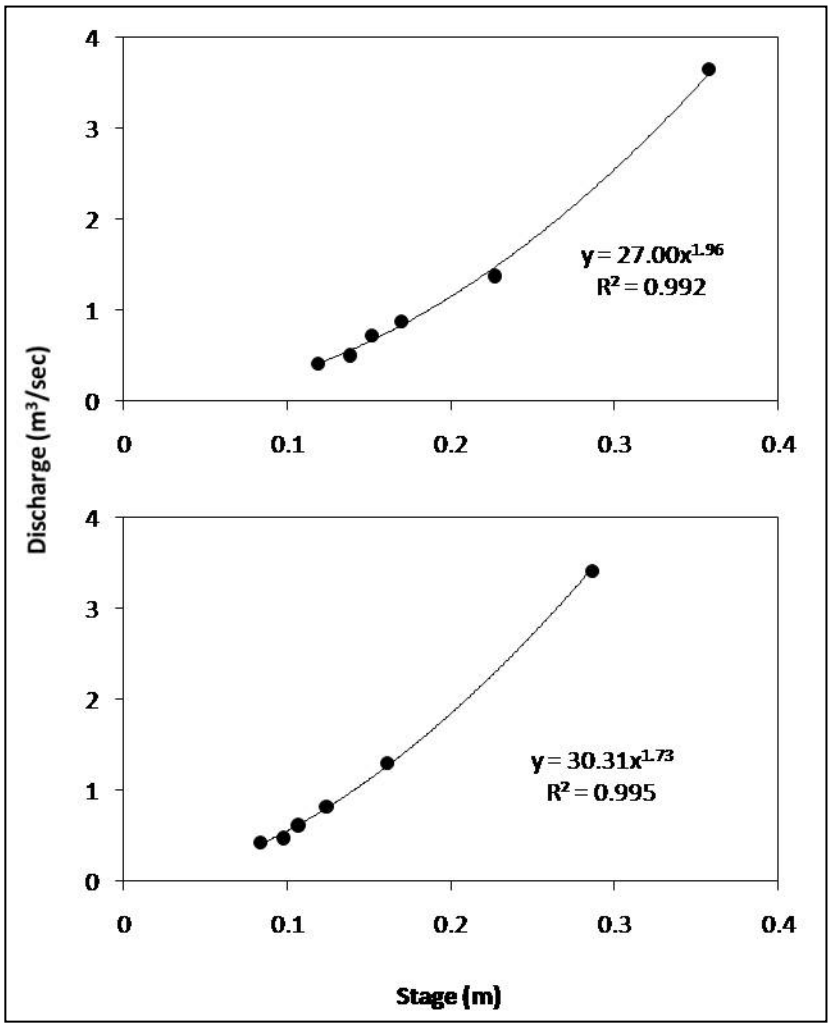
Discharge (m³/sec)
y = 27.00x^1.96
R² = 0.992
y = 30.31x^1.73
R² = 0.995
Stage (m)

Figure 8

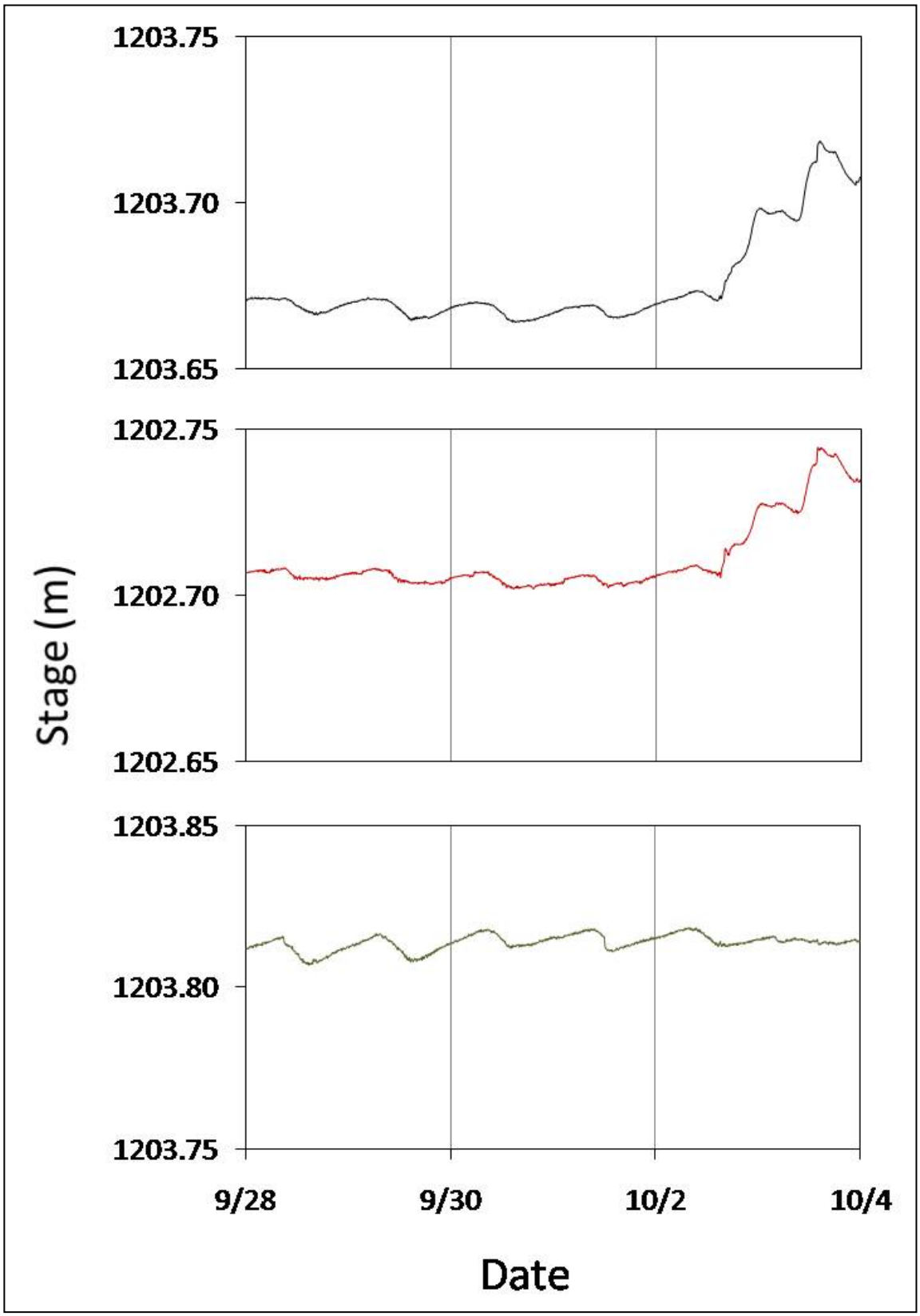
1203.75
1203.70
1203.65
1202.75
1202.70
1202.65
1203.85
1203.80
1203.75
Stage (m)
9/28
9/30
10/2
10/4
Date

Figure 9

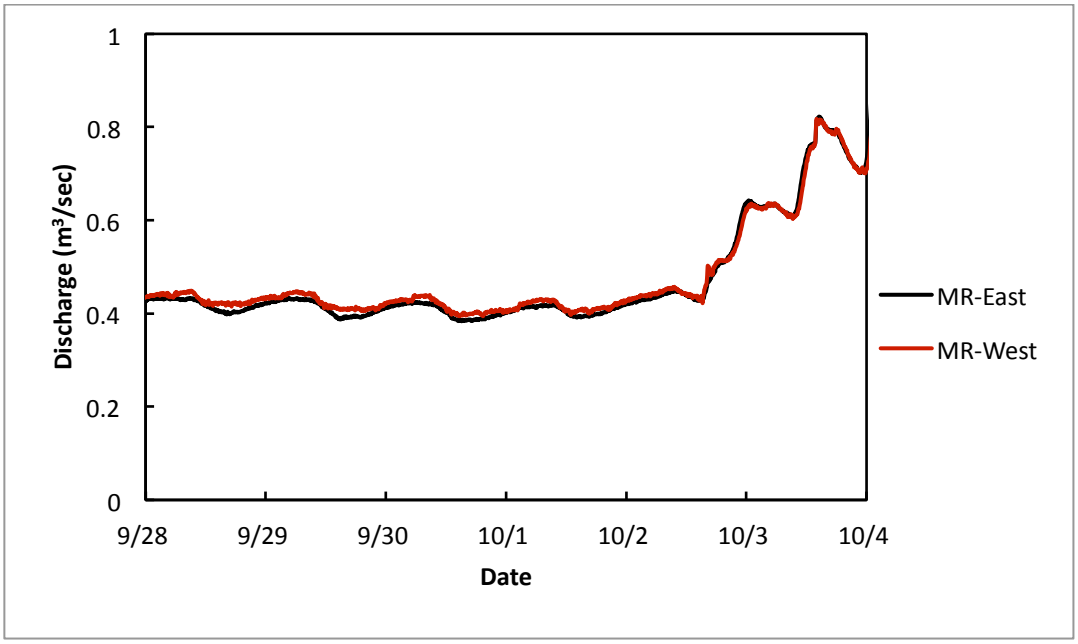

Figure 10

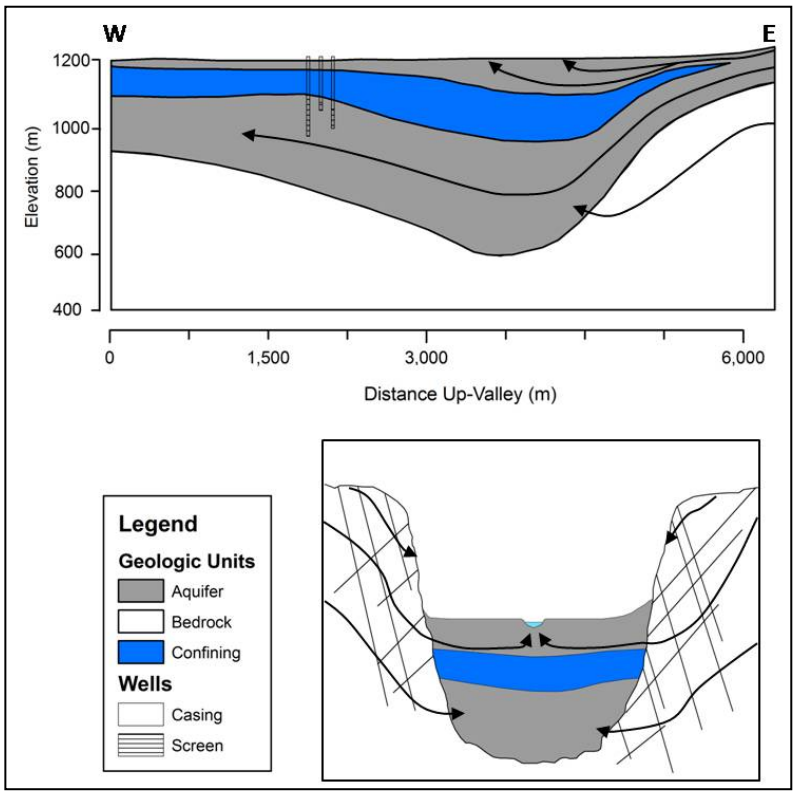

Figure 11

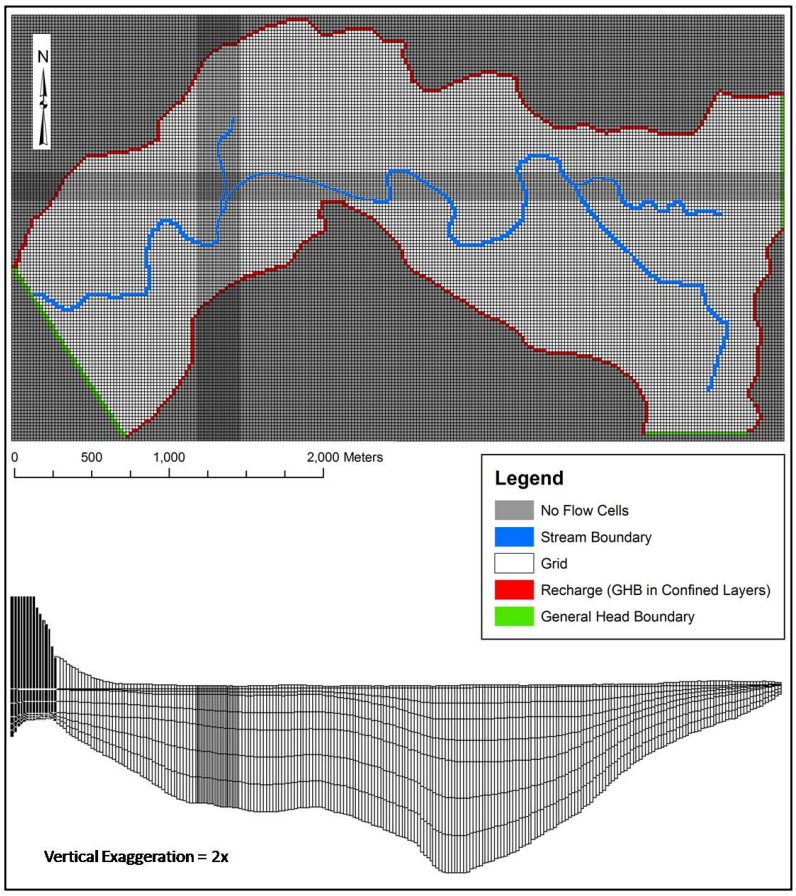

Figure 12

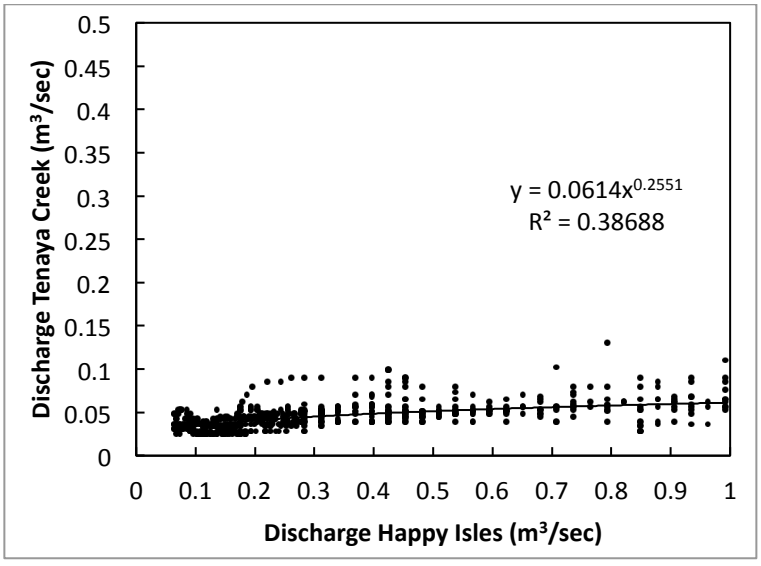

Figure 13

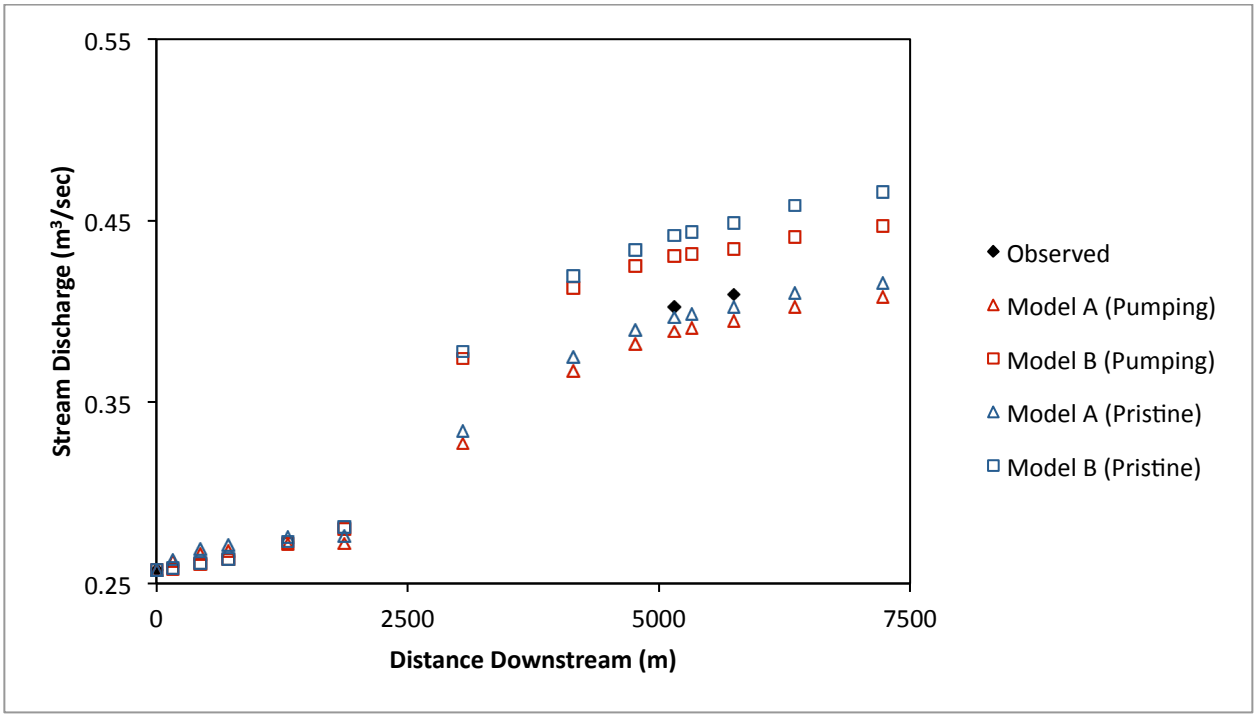

Figure 14

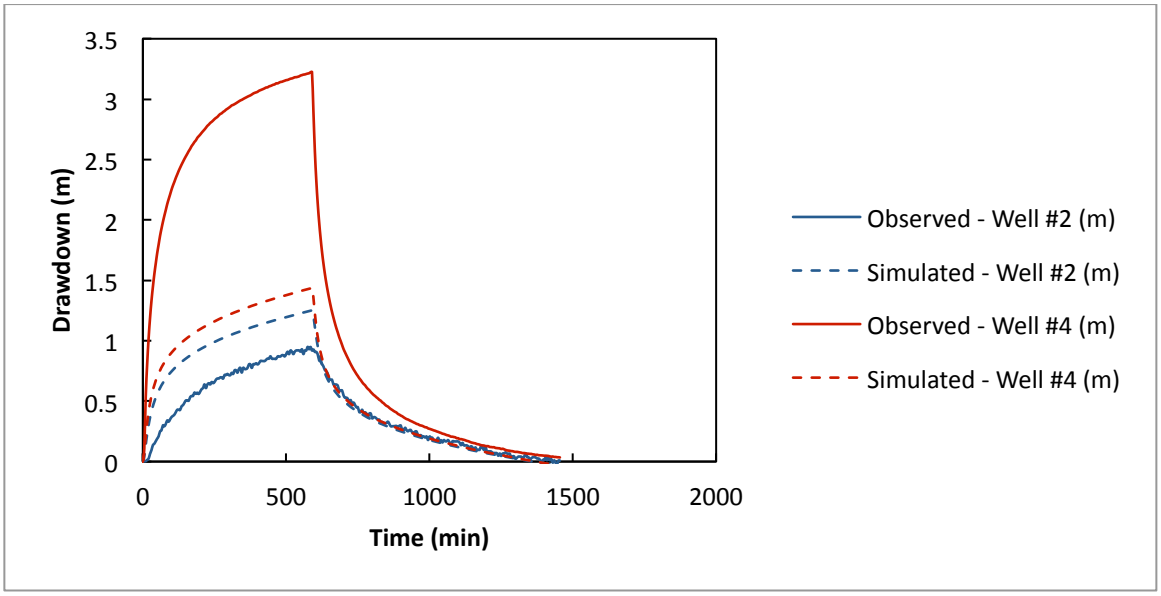

Figure 15

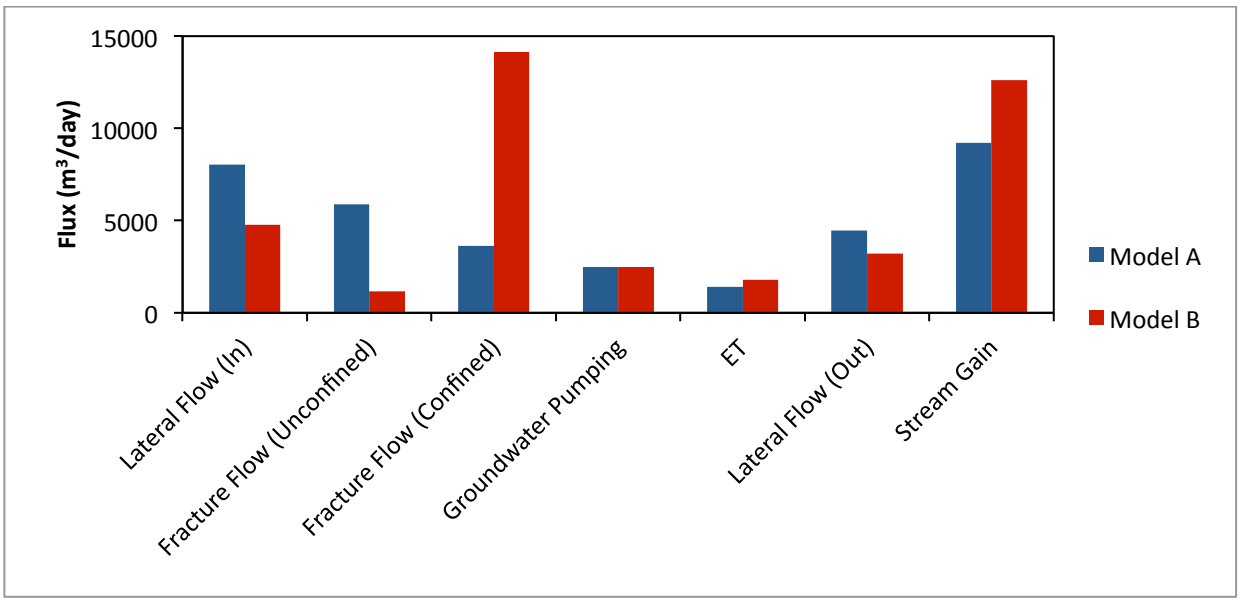

Figure 16

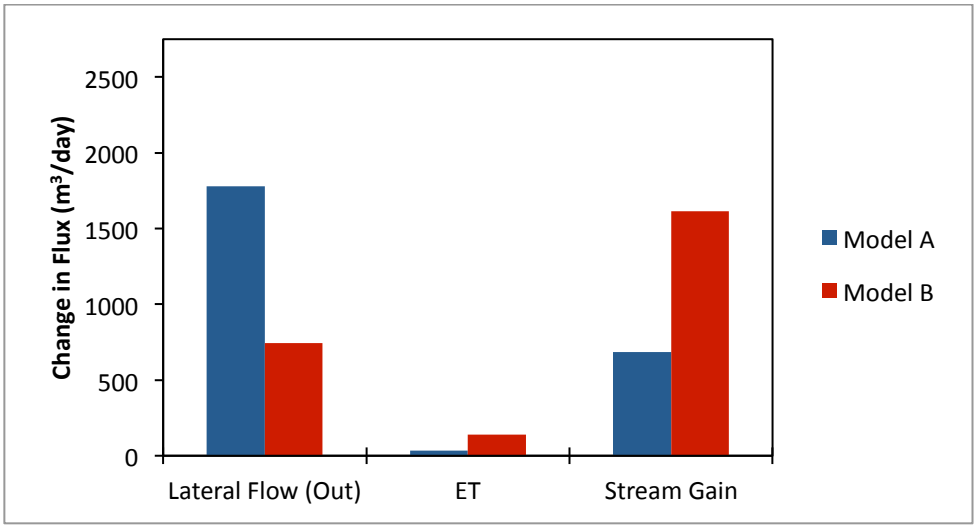

Figure 17

APPENDIX A: PUMPING TEST ANALYSIS

Aquifer properties from the confined units were estimated through the analysis of transient time-drawdown data from groundwater pumping from Well #4 (Test #1) and Well #1 (Test #2). Analysis was conducted using the Theis and methods for non equilibrium radial flow in a confined aquifer (Theis, 1936; Cooper and Jacob, 1946). Drawdown data was recorded in pressure transducers placed in Well #2 and Well #4. Well #1 was not outfitted with a sounding tube and could not be monitored. Due to the limited drawdown (<.05 m) observed in Well #4 in response to pumping in Well #2, we excluded these results from analysis.

Methods

Test #1 was conducted on November 30th, 2010. Pumping at Well #4 began at 8:22am at rate of 4.84 m^3/min and continued for 9 hours and 8 minutes. Drawdown and recovery were recorded at Well #2 at 10 second intervals. Test #2 was conducted on December 6th - 7th, 2010. Pumping at Well #1 began at 7:11pm at a rate of 3.46 m^3/min and continued for 11 hours and 30 minutes. Drawdown and recovery were recorded at Well #2 and Well #4 at 1 minute intervals.

Aquifer parameters were initially estimated using a Theis type curve. Solutions for aquifer transmissivity and storativity were estimated from the Theis equation (Theis, 1936):

$$T = \frac{Q}{4\pi(h_0 - h)} * W(u) \quad (1)$$

$$S = \frac{4Tut}{r^2} \quad (2)$$

where

T is the transmissivity (L^2/T)

S is the storativity (dimensionless)

Q is the pumping rate (L^3/T)

h_0 - h - is the drawdown (L)

t is the time since pumping began (T)

r is the radial distance from the pumping well (L)

u is a dimensionless constant

$W(u)$ is the well function of u (dimensionless)

Additional analysis was conducted using the Cooper-Jacobs Straight-Line Method to provide increased confidence in calculated results. Solutions for aquifer transmissivity and storativity were obtained through the following equations (Cooper and Jacob, 1946):

$$T = \frac{2.3Q}{4\pi\Delta(h_0 - h)} \quad (3)$$

$$S = \frac{2.25Tt_0}{r^2} \quad (4)$$

where

T is the transmissivity (L^2/T)

S is the storativity (dimensionless)

Q is the pumping rate (L^3/T)

$h_0 - h$ is the drawdown (L)

t_0 is the time when the straight-line intersects the zero drawdown axis (T)

r is the radial distance from the pumping well (L)

Results

Maximum observed drawdown at Well #2 was 1.26 m during Test #1 and .95 m during Test #2. Calculated results for aquifer transmissivity and storativity at Well #2 were consistent between Test #1 and Test#2 using both the Theis and Cooper-Jacobs solutions. Aquifer transmissivity values ranged from 1.07 x 10^3 - 1.16 x 10^3 m^2/day and storativity ranged from 1.39 x 10^{-3} - 6.56 x 10^{-3}. Theis curve analysis showed no major deviation from the ideal type-

curve suggesting that drawdown at Well #2 was not significantly affected by recharge or no flow boundaries under the time interval of well pumping.

Maximum drawdown at Well #4 during Test #2 was 3.16 m. Calculated results for aquifer transmissivity ($5.07 \times 10^2 - 5.56 \times 10^2$ m^2/day) and storativity ($3.54 \times 10^{-4} - 4.24 \times 10^{-4}$) were significantly lower than those determined from Well #2 (Table 1). Additionally, plotted field data from Well #4 shows a considerable deviation from the ideal type-curve illustrating the effect of a recharge boundary after approximately 200 minutes of pumping.

Well	Test	Method	T (m2/day)	S
Well #2	November	Theis	1.07E+03	1.70E-03
Well #2	November	Cooper	1.19E+03	1.39E-03
Well #2	December	Theis	1.09E+03	6.56E-03
Well #2	December	Cooper	1.16E+03	4.93E-03
Well #4	December	Theis	5.07E+02	3.54E-04
Well #4	December	Cooper	5.56E+02	4.24E-04

Table 1. Transmissivity and storativity values yielded from aquifer tests using the Cooper-Jacobs and Theis methods

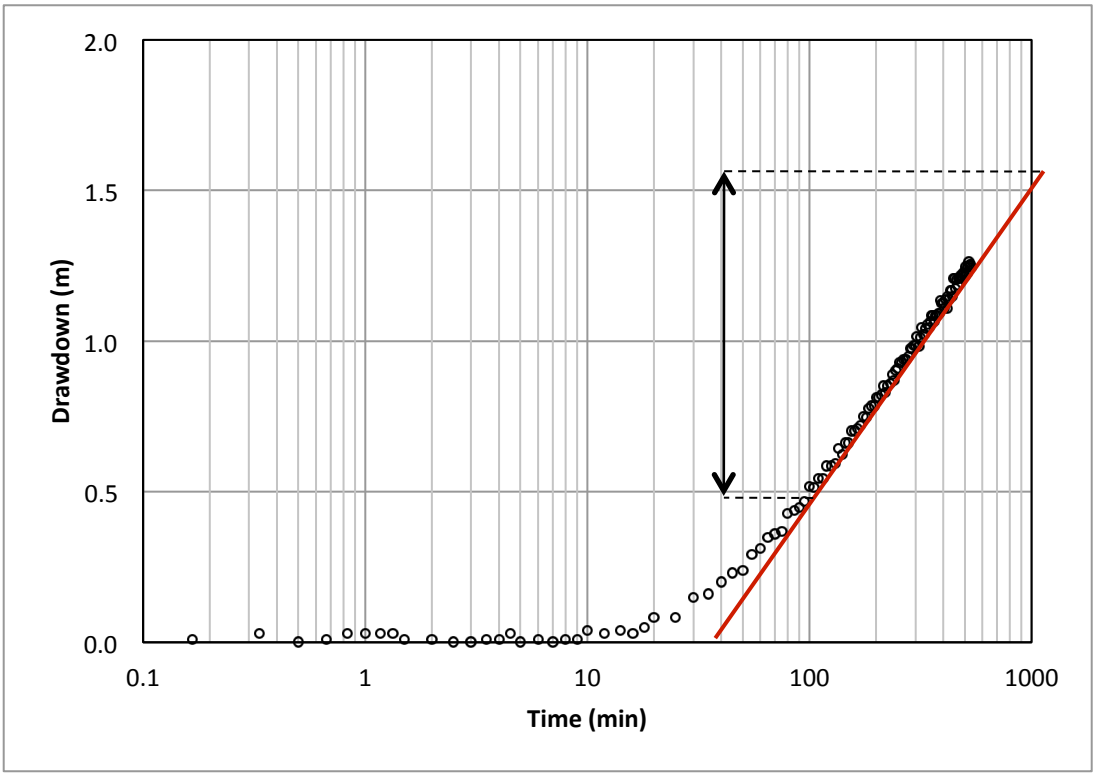

Figure 1. Cooper-Jacob solution for aquifer parameters from drawdown in Well #2 on November 30th 2010

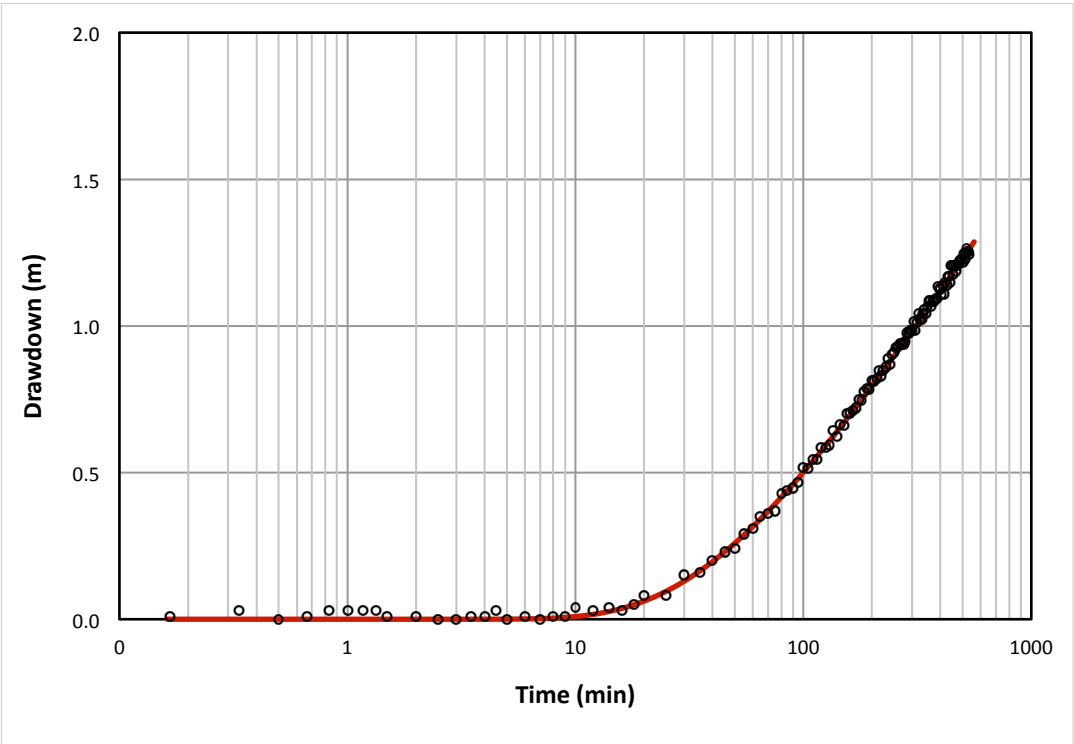

Figure 2. Theis solution for aquifer parameters from drawdown in Well #2 on November 30th 2010

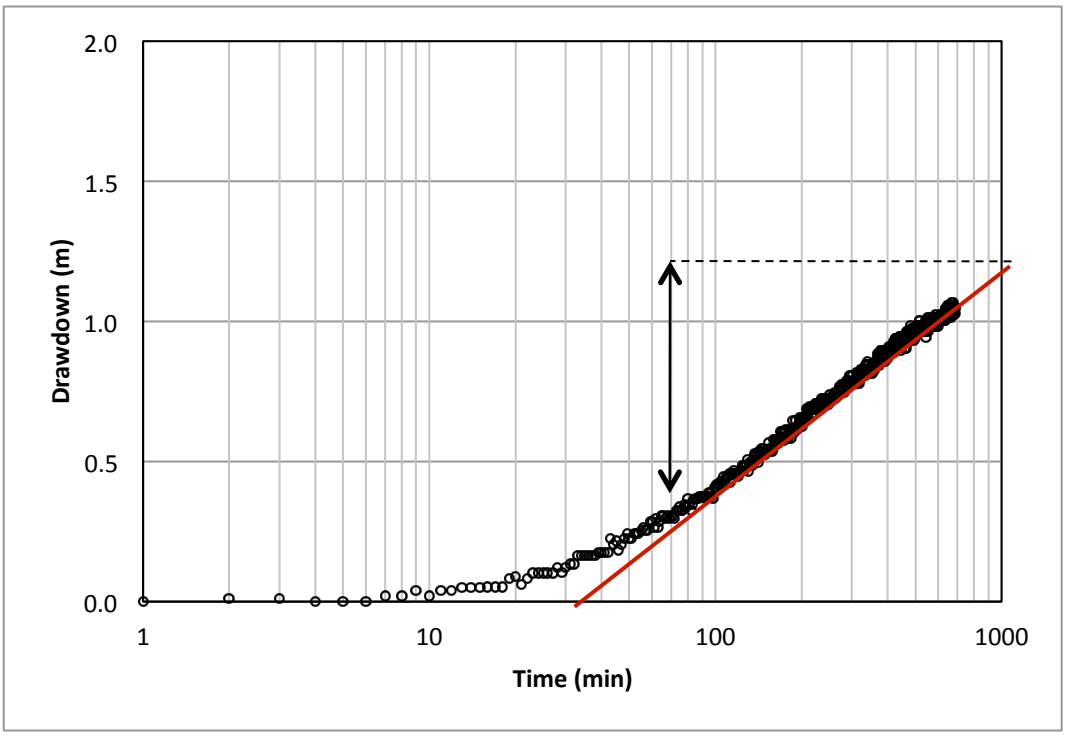

Figure 3. Cooper-Jacob solution for aquifer parameters from drawdown in Well #2 on December 6th – 7th 2010

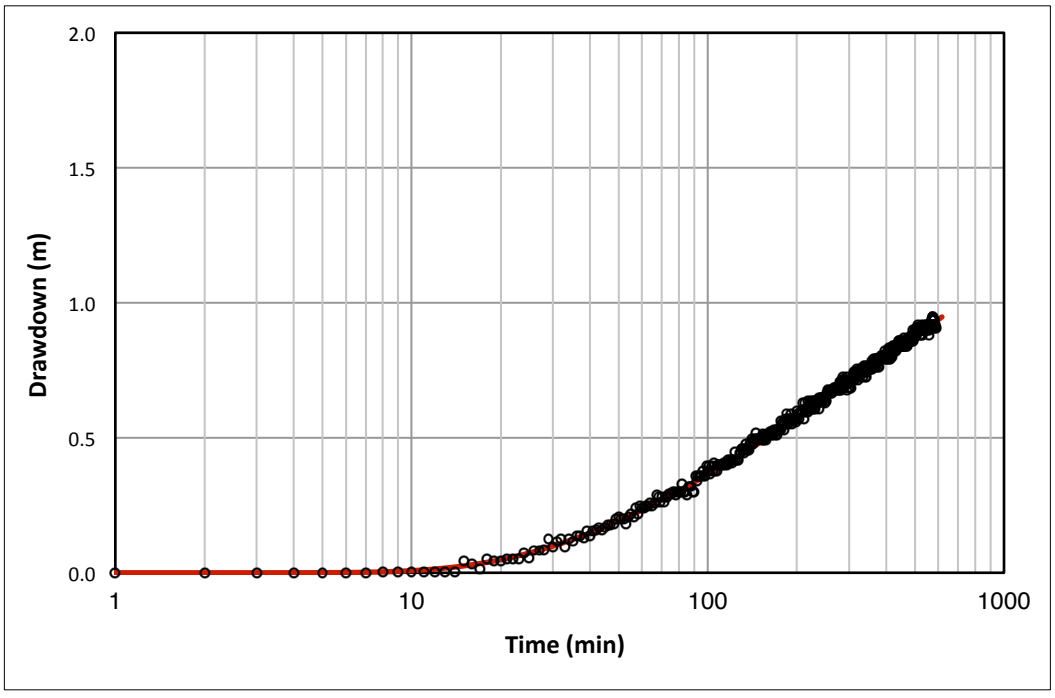

Figure 4. Theis solution for aquifer parameters from drawdown in Well #2 on December 6th – 7th 2010

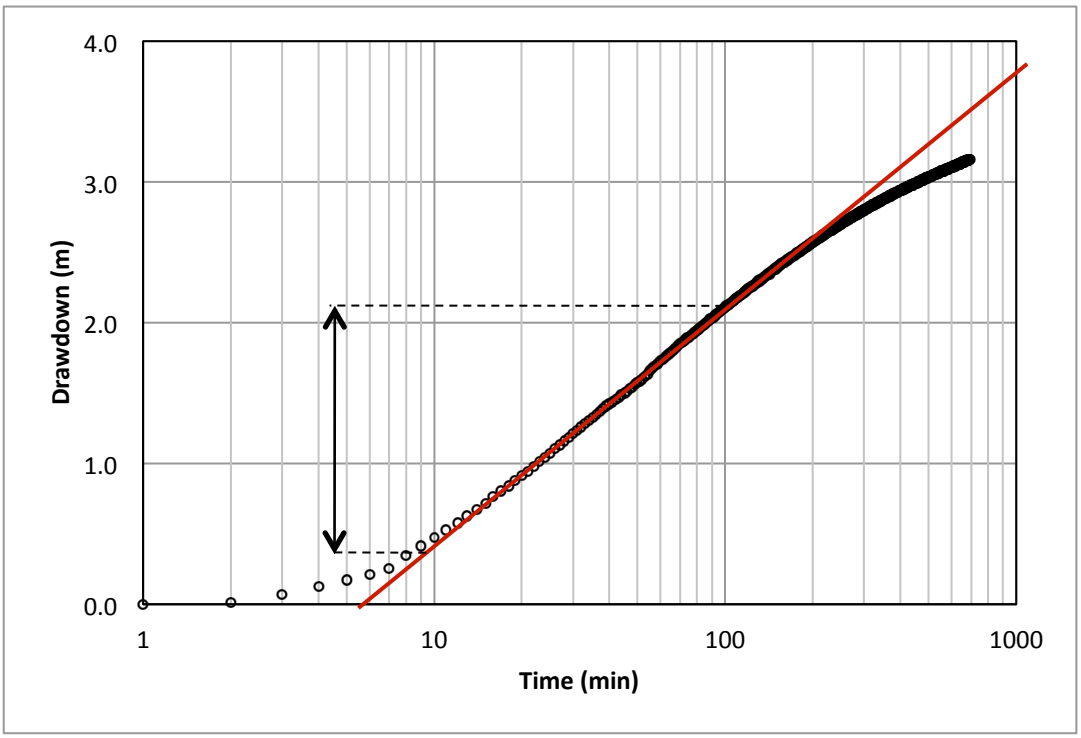

Figure 5. Cooper-Jacob solution for aquifer parameters from drawdown in Well #4 on December 6th – 7th 2010

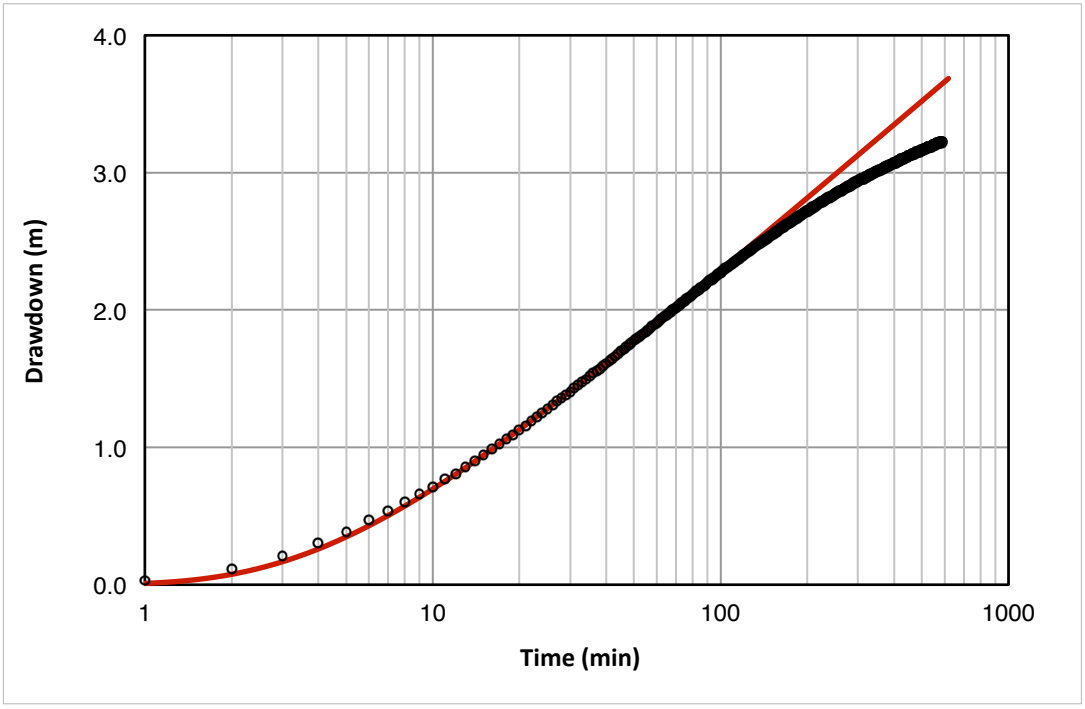

Figure 6. Theis solution for aquifer parameters from drawdown in Well #5 on December 6th – 7th 2010